2023

Classification on Boundary-Equilibria and Singular Continuums of Continuous Piecewise Linear Systems

Hebai Chen

Zhaosheng Feng

Hao Yang

Linfeng Zhou

Classification on Boundary-equilibria and Singular Continuums of Continuous Piecewise Linear Systems

Hebai Chen
Central South University
Zhaosheng Feng (zhaosheng.feng@utrgv.edu)
University of Texas Rio Grande Valley
Hao Yang
Central South University
Linfeng Zhou
Sichuan University

Research Article

Keywords: piecewise linear system, boundary equilibrium, singular continuum, phase portrait, index,

Posted Date: September 28th, 2022

DOI: https://doi.org/10.21203/rs.3.rs-2097867/v1

CLASSIFICATION ON BOUNDARY-EQUILIBRIA AND SINGULAR CONTINUUMS OF CONTINUOUS PIECEWISE LINEAR SYSTEMS

HEBAI CHEN[1], ZHAOSHENG FENG[2], HAO YANG[1], LINFENG ZHOU[3]

Abstract. In this paper, we show that any switching hypersurface of n-dimensional continuous piecewise linear systems is an $(n-1)$-dimensional hyperplane. For two-dimensional continuous piecewise linear systems, we present local phase portraits and indices near the boundary equilibria (i.e., equilibria at the switching line) and singular continuum (i.e., continuum of non-isolated equilibria) between two parallel switching lines. The definition of the index of singular continuum is introduced. Then we show that boundary-equilibria and singular continuums can appear with many parallel switching lines.

1. Introduction

In modern theory of dynamical systems, the study of qualitative properties of equilibrium points has been an interesting topic [7, 20], because it reveals the topological structure of orbits near equilibria and demonstrates dynamical behaviors intuitively. Especially, local phase portraits of hyperbolic equilibria (i.e., no eigenvalue of the associated Jacobian matrices is located at the imaginary axis) persist in the C^0 topology under small nonlinear perturbation by the Hartman-Grobman theorem [20]. In addition to using phase portraits to classify equilibria, we apply the index theory to do classifications of equilibria for ordinary differential equations. Some applications of these two approaches to isolated equilibria and singular lines of planar linear systems can be seen in [7, 20].

Recently, considerable attention has been attracted to dynamical behaviors of nonsmooth dynamical systems, since nonsmooth dynamical systems have tremendous applications in control engineering and mechanics, economics, climate modelling, physiological modelling, medicine, ecology and epidemiology, see [1, 2, 11]. As shown in [1, 2, 10, 12], there are a number of nonsmooth systems with the parameters which display bifurcations at certain parametric values. However, their phase portraits are topologically equivalent in certain regions. Hence, classifications of boundary-equilibria and singular continuums by phase portraits can provide useful dynamical information of nonsmooth dynamical systems. The index of an equilibrium is another quantity to characterize the topological structure of equilibrium. Moreover, the study of an equilibrium can help us to better understand the existence of limit cycles since the sum of the indices of all equilibria surrounded by a limit cycle is 1. As we see, the planar continuous piecewise linear system with the switching lines is actually the simplest nonsmooth dynamical system. For some results of continuous piecewise linear systems we refer to [1, 5, 6, 15, 16, 17, 18, 19] and for some boundary equilibria and singular continuums of continuous piecewise linear systems we refer to [3, 4, 9, 14]. As far as our knowledge goes, there are no complete classifications on phase portraits of boundary-equilibria and singular continuums for continuous

2010 *Mathematics Subject Classification.* Primary 34C05; 34A26; 49J52.
Key words and phrases. piecewise linear system; boundary equilibrium; singular continuum; phase portrait; index.

piecewise linear systems. Furthermore, it does not seem that the definition of the index of singular continuum was presented previously in the literature. The aim of this paper is to discuss and demonstrate a complete classification of boundary-equilibria and singular continuums of continuous piecewise linear systems.

The outline of this paper is given as follows. In Section 2, we recall some related results on phase portraits and indices of the interior equilibria for smooth linear systems and use them to show that these equilibria are not located at a switching manifold of nonsmooth linear systems. After presenting phase portraits, indices of equilibria and singular continuum in Sections 3 and 4 respectively, we rigorously prove that any switching line of continuous piecewise linear systems must be a straight line.

2. Phase portraits and indices of interior equilibria

In this section, we briefly present phase portraits and indices of the interior equilibria, i.e., the equilibria do not lie on the switching manifold which are the same as the ones for smooth linear systems.

We start with the classification and index of an equilibrium of linear systems [7, 13, 20]. To define the index of an equilibrium, we recall the definition of rotation number of an oriented close curve with respect to a continuous vector field [20].

Consider a continuous planar differential equation

$$\frac{dx}{dt} = X(x,y), \quad \frac{dy}{dt} = Y(x,y). \tag{1}$$

Let $A(x,y) := (X(x,y), Y(x,y))$ and $\mathscr{L} \subset \mathbb{R}^2$ be a piecewise smooth oriented close curve. For any fixed oriented Jordan curve $\mathscr{L} \subset \mathbb{R}^2$, the rotation number of $\mathscr{L}$ with respect to $A(x,y)$, denoted by $\gamma(A(x,y), \mathscr{L})$, is given by

$$\gamma(A(x,y), \mathscr{L}) := \frac{\Delta_{\mathscr{L}}}{2\pi},$$

where $\Delta_{\mathscr{L}}$ is the net change of the vector $A(x,y)$ as (x,y) traverses the loop in the positive direction. Suppose that $P_0(x_0,y_0)$ is an isolated critical point of system (1). We know that there is a value $R > 0$ such that for any $0 < r < R$, the rotation number $\gamma\left(A(x,y), \partial S\left(P_0, r\right)\right)$ is a constant independent of r (see [20, p.147]), where $S\left(P_0, r\right) := \{(x,y) \in \mathbb{R}^2 : \sqrt{(x-x_0)^2 + (y-y_0)^2} \leq r\}$, the open ball of radius r centered at P_0, contains only one equilibrium P_0 of system (1), and $\partial S\left(P_0, r\right)$ denotes the boundary of $S\left(P_0, r\right)$.

Definition 1. [20, p.147] *For the continuous system* (1)*, we suppose that* $P_0(x_0,y_0)$ *is an isolated critical point of system* (1) *and* r *is a small positive constant. The rotation number* $\gamma\left(A(x,y), \partial S\left(P_0, r\right)\right)$ *is called the index of the critical point* P_0 *for system* (1)*.*

For an interior equilibrium, the continuous planar linear system can be written as

$$\dot{x} = \begin{cases} b_1 x + a_2 y, & \text{if } -\varepsilon \leq x < a, \\ a_1 x + a_2 y, & \text{if } a \leq x < a + \varepsilon, \end{cases} \quad \dot{y} = \begin{cases} b_2 x + a_4 y, & \text{if } -\varepsilon \leq x < a, \\ a_3 x + a_4 y, & \text{if } a \leq x < a + \varepsilon, \end{cases} \tag{2}$$

where $a > 0$, $\epsilon > 0$ is very small, $a_i, b_i \in \mathbb{R}$ for $i = 1,2,3,4$ and ${b_1}^2 + {a_2}^2 + {b_2}^2 + {a_4}^2 \neq 0$. Moreover, the Jordan canonical forms of

$$A := \begin{pmatrix} b_1 & a_2 \\ b_2 & a_4 \end{pmatrix}$$

have three cases

$$J_1 := \begin{pmatrix} \lambda & 0 \\ 0 & \mu \end{pmatrix}, \quad J_2 := \begin{pmatrix} \lambda & 1 \\ 0 & \lambda \end{pmatrix}, \quad J_3 := \begin{pmatrix} a & b \\ -b & a \end{pmatrix}, \tag{3}$$

where $\lambda^2 + \mu^2 \neq 0$ and $b \neq 0$.

Note that λ, μ cannot be zero simultaneously. Without loss of generality, we only consider the case $\lambda \geq \mu$ when $A = J_1$, because the transformation $(x, y, \lambda, \mu) \to (y, x, \mu, \lambda)$ can convert the case $\lambda \leq \mu$ to the case $\lambda \geq \mu$.

Theorem 1. [20, Chapter 3] *Given system* (2) *with the three Jordan canonical forms* (3)*, local phase portraits at equilibria are shown in* Figure 1.

Specifically, when $A = J_1$, in the cases $\mu = 0$, $\lambda\mu < 0$, $\lambda > \mu > 0$ and $\lambda = \mu > 0$, system (2) *has a singular line $x = 0$, a unique equilibrium which is a saddle, a unique equilibrium which is a bidirectional node, and a unique equilibrium which is a star node, respectively. Phase portraits of system* (2) *are shown in Figure 1(a)-1(d), respectively.*

When $A = J_2$, in the cases $\lambda = 0$ and $\lambda > 0$, system (2) *has a singular line $y = 0$ and a unique equilibrium which is a unidirectional node respectively. Phase portraits of system* (2) *are shown in Figure 1(e) and 1(f), respectively.*

When $A = J_3$, in the cases $a = 0, b > 0$ and $a > 0, b > 0$, system (2) *has a unique equilibrium which is a center and a unique equilibrium which is a focus, respectively. Phase portraits of system* (2) *are shown in Figure 1(g) and 1(h), respectively.*

Moreover, the index of the saddle is -1 and the index of a bidirectional node, or star node, or unidirectional node, or center, or focus is 1.

Remark 1. *Considering $A = J_1$, we do not mention the case $0 > \lambda > \mu$, since we can use the transformation $(\lambda, \mu, t) \to -(\lambda, \mu, t)$ to change the case $0 > \lambda > \mu$ to the case $\mu > \lambda > 0$. For $A = J_2$, we do not include the case $\lambda < 0$, since we can use the transformation $(t, \lambda) \to -(t, \lambda)$ to change the case $\lambda < 0$ to the case $\lambda > 0$. Similarly, for $A = J_3$, we do not mention the cases $a = 0$, $b < 0$; $a > 0$, $b < 0$; $a < 0$, $b > 0$; and $a < 0$, $b < 0$.*

3. Phase portraits and indices of boundary-equilibria

In this section, we study phase portraits and indices of isolated equilibria for continuous piecewise linear systems at a switching line. Note that the boundaries between two different linear zones of piecewise linear systems are responsible for the non-smoothness of vector fields, so we call this boundary as the switching curve of the system.

Proposition 2. *A switching curve of continuous piecewise linear systems is a straight line.*

Proof. We consider a local region $\mathcal{D} \subset \mathbb{R}^2$ of phase space that only contains one switching line. Without loss of generality, a continuous piecewise linear system in the neighborhood $\mathcal{D}$ of the switching line can be rewritten in the form

$$\begin{aligned} \dot{x} &= \begin{cases} b_1 x + b_2 y + c_1, & \text{if } F(x, y) < 0, \\ a_1 x + a_2 y + c_2, & \text{if } F(x, y) > 0, \end{cases} \\ \dot{y} &= \begin{cases} b_3 x + b_4 y + c_3, & \text{if } F(x, y) < 0, \\ a_3 x + a_4 y + c_4, & \text{if } F(x, y) > 0, \end{cases} \end{aligned} \tag{4}$$

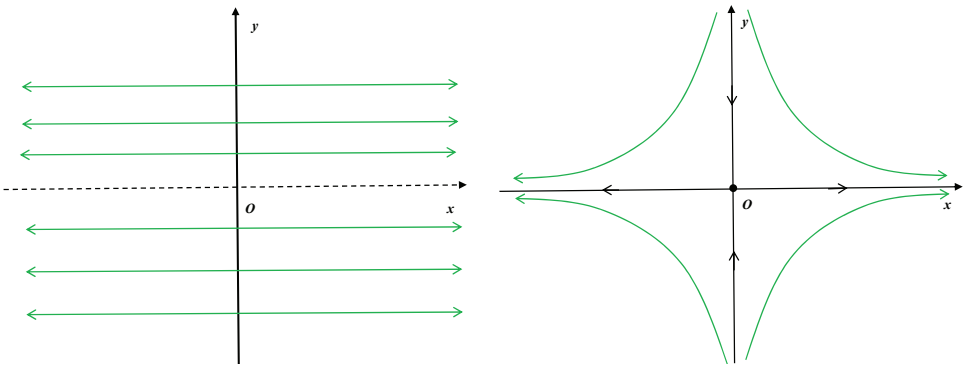

(a) A singular line $x = 0$

(b) A saddle

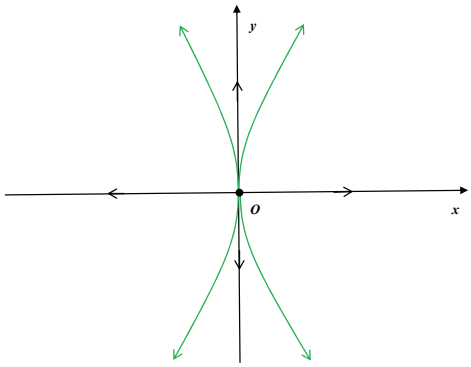

(c) A bidirectional node

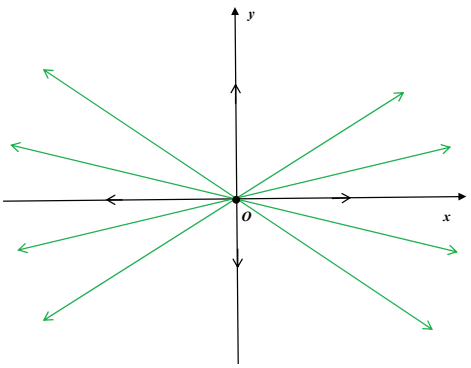

(d) A star node

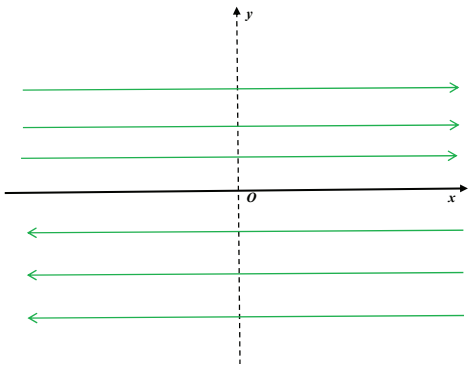

(e) A singular line $y = 0$

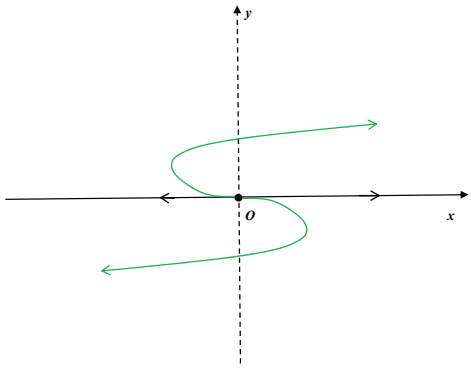

(f) A unidirectional node

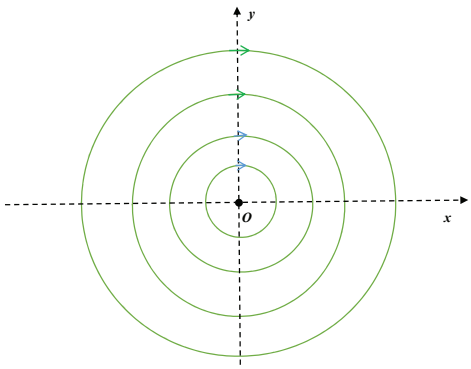

(g) A center

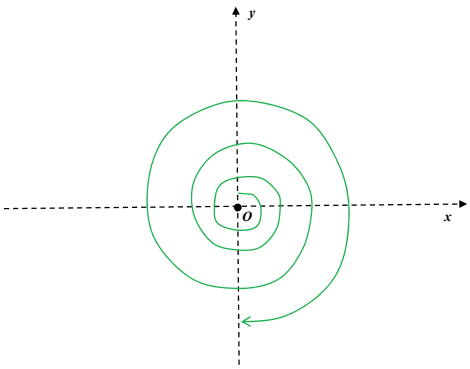

(h) A focus

Figure 1. Classification of an equilibrium in the linear system (2)

where $(a_1, \ldots, a_4, b_1, \ldots, b_4, c_1, \ldots, c_4) \in \mathbb{R}^{12}$ and $F : \mathbb{R}^2 \mapsto \mathbb{R}$ is a continuous scalar function of $(x, y) \in \mathcal{D}$.

Let (x_0, y_0) be on the switching line $F(x, y) = 0$. Since the vector field of system (4) is continuous, we obtain

$$\begin{cases} b_1 x_0 + b_2 y_0 + c_1 \equiv a_1 x_0 + a_2 y_0 + c_2, \\ b_3 x_0 + b_4 y_0 + c_3 \equiv a_3 x_0 + a_4 y_0 + c_4 \end{cases}$$

for all $(x_0, y_0) \in \{(x, y) \in \mathcal{D} : F(x, y) = 0\}$. $F(x, y) = 0$ is not a straight line, if and only if $c_1 = c_2$, $c_3 = c_4$ and $a_i = b_i$ $(i = 1, 2, 3, 4)$. In other words, system (4) is linear, implying that the curve $F(x, y) = 0$ is not a switching line. Clearly, this is a contradiction. □

Remark 2. *By using a similar approach we can see that the result described in Proposition 2 also holds for continuous piecewise linear systems in $\mathbb{R}^n$, i.e., the switching hypersurface is actually an $(n-1)$-dimensional hyperplane.*

Now we are ready to study the qualitative properties of boundary-equilibria. We consider a local region $\mathcal{D}_1 \subset \mathbb{R}^2$ of phase space that contains just one switching line and the origin. Without loss of generality, a boundary-equilibrium lies at the origin and continuous piecewise linear systems in $\mathcal{D}_1$ can be transformed to

$$\dot{x} = \begin{cases} b_1 x + a_2 y, & \text{if } x < 0, \\ a_1 x + a_2 y, & \text{if } x > 0, \end{cases} \quad \dot{y} = \begin{cases} b_2 x + a_4 y, & \text{if } x < 0, \\ a_3 x + a_4 y, & \text{if } x > 0, \end{cases} \tag{5}$$

where $(a_1, a_2, a_3, a_4, b_1, b_2) \in \mathbb{R}^6$, $(x, y) \in \mathcal{D}_1$, $a_4 b_1 - a_2 b_2 \neq 0$, and $a_1 a_4 - a_2 a_3 \neq 0$. For system (5), we only consider $a_2 \geq 0$. Otherwise, if $a_2 < 0$, we can derive the similar result through the transformation $(y, a_2, a_3, b_2) \to -(y, a_2, a_3, b_2)$. Moreover, $a_1 = b_1$ and $a_3 = b_2$ cannot hold simultaneously, since system (5) is a linear system and $x = 0$ is not a switching line if $a_1 = b_1$ and $a_3 = b_2$.

The switching line $x = 0$ separates $\mathcal{D}_1$ into three regions

$$\mathcal{S}_l := \{(x, y) \in \mathcal{D}_1 : x < 0\}, \quad \mathcal{S}_r := \{(x, y) \in \mathcal{D}_1 : x > 0\}, \quad \Sigma_c := \{(x, y) \in \mathcal{D}_1 : x = 0\}.$$

Let $\mathcal{D}_1 := \mathcal{S}_l \cup \Sigma_c \cup \mathcal{S}_r$. Then the Jacobian matrices in the zones $\mathcal{S}_l$ and $\mathcal{S}_r$ are

$$J_l := \begin{pmatrix} b_1 & a_2 \\ b_2 & a_4 \end{pmatrix}, \; J_r := \begin{pmatrix} a_1 & a_2 \\ a_3 & a_4 \end{pmatrix},$$

respectively. For simplicity, let $D_1 := \det J_l = a_4 b_1 - a_2 b_2$, $D_2 := \det J_r = a_1 a_4 - a_2 a_3$, $T_1 := \mathrm{tr} J_l = a_4 + b_1$, $T_2 := \mathrm{tr} J_r = a_1 + a_4$, $\Delta_1 := {T_1}^2 - 4D_1$ and $\Delta_2 := {T_2}^2 - 4D_2$.

Dynamical behavior of system (5) at $\mathcal{S}_l$ (resp. $\mathcal{S}_r$) is saddle type when $D_1 < 0$ (resp. $D_2 < 0$), node type when $D_1 > 0$ and $\Delta_1 \geq 0$ (resp. $D_2 > 0$ and $\Delta_2 \geq 0$), focus type when $T_1 \neq 0$, $D_1 > 0$ and $\Delta_1 < 0$ (resp. $T_2 \neq 0$, $D_2 > 0$ and $\Delta_2 < 0$), center type when $D_1 > 0$ and $T_1 = 0$ (resp. $D_2 > 0$ and $T_2 = 0$). Further, we call that the origin of system (5) is a boundary-saddle point (resp., boundary-node point) if dynamical behaviors of system (5) at $\mathcal{S}_l$ and $\mathcal{S}_r$ are saddle (resp., node). Moreover, we call that the origin of system (5) is a boundary-focus point (resp., boundary-center point) if the origin of system (5) is still a focus (resp. center). We can also define saddle-node point, saddle-focus point, saddle-center point, node-focus point, and node-center point in a similarly manner.

3.1. **Boundary-saddle point.** Local phase portraits at the boundary-saddle points can be summarized by the following theorem.

Theorem 3. *Suppose that $D_1 < 0$ and $D_2 < 0$ for system (5). When $a_2 = 0$, system (5) is topologically equivalent to*

$$\dot{x} = \begin{cases} \tilde{b}_1 x, & \text{if } x < 0, \\ \tilde{a}_1 x, & \text{if } x > 0, \end{cases} \quad \dot{y} = y, \tag{6}$$

where $\tilde{a}_1$, $\tilde{b}_1 < 0$ with $\tilde{a}_1 \neq \tilde{b}_1$. Local phase portrait at the boundary-saddle point is shown in Figure 2.

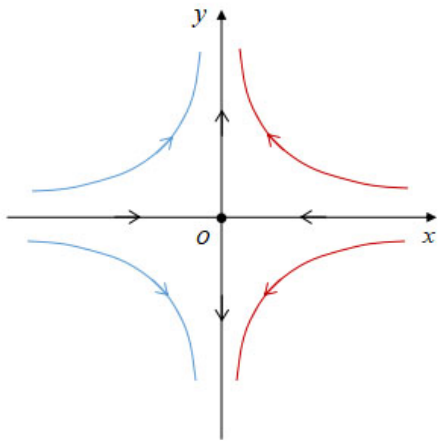

Figure 2. Local phase portrait at the boundary-saddle point of system (6)

When $a_2 > 0$, system (5) is topologically equivalent to

$$\dot{x} = \begin{cases} \tilde{b}_1 x + y, & \text{if } x < 0, \\ \tilde{a}_1 x + y, & \text{if } x > 0, \end{cases} \quad \dot{y} = \begin{cases} \tilde{b}_2 x, & \text{if } x < 0, \\ \tilde{a}_3 x, & \text{if } x > 0, \end{cases} \tag{7}$$

where $(\tilde{a}_1, \tilde{b}_1) \in \mathbb{R}^2$ and $\tilde{a}_3$, $\tilde{b}_2 > 0$. Local phase portrait at the boundary-saddle point is shown in Figure 3.

Proof. For $a_2 = 0$, from $D_1 < 0$ and $D_2 < 0$ it follows that

$$a_1 a_4 < 0, \quad b_1 a_4 < 0.$$

In the zone $\mathcal{S}_l$, with the transformation

$$(y, t) \to \left(y + \frac{b_2}{b_1 - a_4} x, \ \frac{t}{a_4} \right),$$

system (5) is changed into (6), where $\tilde{b}_1 = b_1/a_4 < 0$. In the zone $\mathcal{S}_r$, with the transformation

$$(y, t) \to \left(y + \frac{a_3}{a_1 - a_4} x, \ \frac{t}{a_4} \right),$$

system (5) is changed into (6), where $\tilde{a}_1 = a_1/a_4 < 0$.

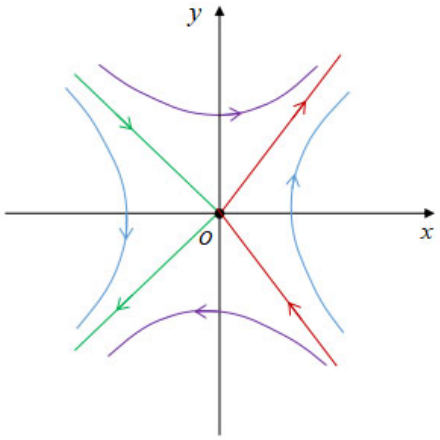

Figure 3. Local phase portrait at the boundary-saddle point of system (7).

For $a_2 > 0$, we use the transformation $(y, t) \to (y + a_4/a_2 x, t/a_2)$ to change system (5) into (7), where $\tilde{b}_1 = T_1/a_2$, $\tilde{b}_2 = -D_1/a_2^2$, $\tilde{a}_1 = T_2/a_2$ and $\tilde{a}_3 = -D_2/a_2^2$. Note that $\tilde{a}_3$, $\tilde{b}_2 > 0$ due to $D_1 < 0$ and $D_2 < 0$.

According to Theorem 1, we can obtain the local phase portrait at the boundary-saddle point of system (6) as shown in Figure 2 and the local phase portrait at the boundary-saddle point of system (7) as shown in Figure 3. □

3.2. **Saddle-node point.** Local phase portraits at the saddle-node point of system (5) can be summarized in the following theorem.

Theorem 4. *Suppose that $D_1 < 0$, $D_2 > 0$ and $\Delta_2 \geq 0$ for system (5). When $a_2 = 0$, system (5) is topologically equivalent to*

$$\dot{x} = \begin{cases} \tilde{b}_1 x, & \text{if } x < 0, \\ \tilde{a}_1 x, & \text{if } x > 0, \end{cases} \quad \dot{y} = \begin{cases} y, & \text{if } x < 0, \\ \tilde{a}_3 x + y, & \text{if } x > 0, \end{cases} \tag{8}$$

where $\tilde{b}_1 < 0$, $\tilde{a}_1 > 0$, $\tilde{a}_3 = 0$ if $\tilde{a}_1 \neq 1$ and $\tilde{a}_3 \geq 0$ if $\tilde{a}_1 = 1$. Local phase portraits at the saddle-node point of system (8) are presented in Figure 4.

When $a_2 > 0$, system (5) is topologically equivalent to

$$\dot{x} = \begin{cases} \tilde{b}_1 x + y, & \text{if } x < 0, \\ \tilde{a}_1 x + y, & \text{if } x > 0, \end{cases} \quad \dot{y} = \begin{cases} \tilde{b}_2 x, & \text{if } x < 0, \\ \tilde{a}_3 x, & \text{if } x > 0, \end{cases} \tag{9}$$

where $\tilde{b}_1 \in \mathbb{R}$, $\tilde{b}_2 > 0$, and $\tilde{a}_1 \geq 2\sqrt{-\tilde{a}_3}$ with $\tilde{a}_3 < 0$. Local phase portraits at the saddle-node point of system (9) are presented in Figure 5.

Proof. For $a_2 = 0$, from $D_1 < 0$, $D_2 > 0$ and $\Delta_2 \geq 0$ it follows that

$$a_1 a_4 > 0, \quad b_1 a_4 < 0.$$

In the zone $\mathcal{S}_l$, with the transformation

$$(y, t) \to \left(y + \frac{b_2}{b_1 - a_4} x, \ \frac{t}{a_4} \right),$$

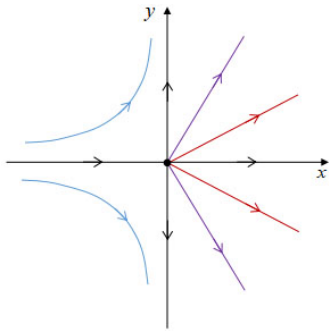

(a) $\tilde{a}_1 = 1$, $\tilde{a}_3 = 0$

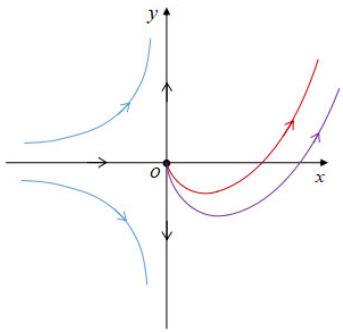

(b) $\tilde{a}_1 = 1$, $\tilde{a}_3 > 0$

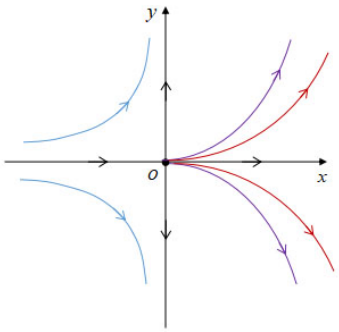

(c) $\tilde{a}_1 > 1$, $\tilde{a}_3 = 0$

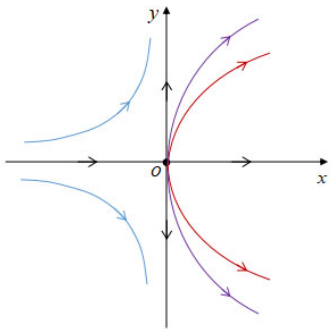

(d) $\tilde{a}_1 \in (0, 1)$, $\tilde{a}_3 = 0$

Figure 4. Local phase portraits at the saddle-node points of system (8).

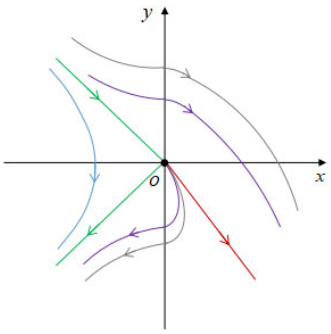

(a) $\tilde{a}_1 = 2\sqrt{-\tilde{a}_3}$, $\tilde{a}_3 < 0$

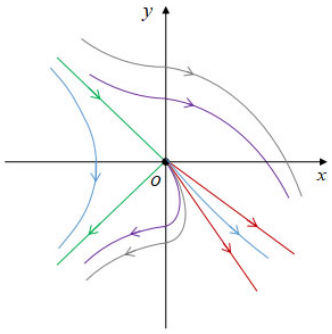

(b) $\tilde{a}_1 > 2\sqrt{-\tilde{a}_3}$, $\tilde{a}_3 < 0$

Figure 5. Local phase portraits of the saddle-node points of system (9).

system (5) is changed into (8), where $\tilde{b}_1 = b_1/a_4 < 0$. In the zone $\mathcal{S}_r$, when $a_1 = a_4$, by a scaling $t \to t/a_4$, system (5) is changed into (8), where $\tilde{a}_1 = 1$ and $\tilde{a}_3 = a_3/a_4$. Note that system (8) is invariant under the transformation $(y, \tilde{a}_3) \to (-y, -\tilde{a}_3)$. Hence, we only consider the non-negative $\tilde{a}_3$. When $a_1 \neq a_4$, in the zone $\mathcal{S}_r$, with the transformation

$$(y, t) \to \left(y + \frac{a_3}{a_1 - a_4} x, \ \frac{t}{a_4} \right),$$

system (5) is changed into (8), where $\tilde{a}_1 = a_1/a_4 \in (0,1)\cup(1,+\infty)$ and $\tilde{a}_3 = 0$. Note that $\tilde{a}_1 > 1$ for $|a_1| > |a_4|$ and $\tilde{a}_1 \in (0,1)$ for $|a_1| < |a_4|$. Thus, local phase portraits at the saddle-node points of systems (8) can be derived from Theorem 1 as shown in Figure 4.

When $a_2 > 0$, from $D_1 < 0$, $D_2 > 0$ and $\Delta_2 \geq 0$ it follows that

$$T_2 = a_1 + a_4 \in (-\infty - 2\sqrt{D_2}] \cup [2\sqrt{D_2}, +\infty).$$

In the zones $\mathcal{S}_l$ and $\mathcal{S}_r$, we use the transformation $(y,t) \to (y + a_4/a_2 x, t/a_2)$ to change system (5) into (9), where $\tilde{b}_1 = T_1/a_2$, $\tilde{b}_2 = -D_1/a_2^2$, $\tilde{a}_1 = T_2/a_2 \in (-\infty - 2\sqrt{D_2}/a_2] \cup [2\sqrt{D_2}/a_2, +\infty)$ and $\tilde{a}_3 = -D_2/a_2^2$. Note that system (9) is invariant under the transformation $(y,t,\tilde{a}_1,\tilde{b}_1) \to -(y,t,\tilde{a}_1,\tilde{b}_1)$. Hence, we only need to consider that $\tilde{a}_1 \in [2\sqrt{D_2}/a_2, +\infty)$. Therefore, by virtue of Theorem 1 we can obtain local phase portraits at the saddle-node points of system (9) as shown in Figure 5. □

3.3. **Saddle-focus/center point.** We consider local phase portraits at the saddle-focus/center points in this subsection.

Theorem 5. *Suppose that $D_1 < 0$, $D_2 > 0$ and $\Delta_2 < 0$ for system (5). Then system (5) is topologically equivalent to*

$$\dot{x} = \begin{cases} \tilde{b}_1 x + y, & \text{if } x < 0, \\ \tilde{a}_1 x + y, & \text{if } x > 0, \end{cases} \qquad \dot{y} = \begin{cases} \tilde{b}_2 x, & \text{if } x < 0, \\ \tilde{a}_3 x, & \text{if } x > 0, \end{cases} \tag{10}$$

where $\tilde{b}_1 \in \mathbb{R}$, $\tilde{b}_2 > 0$, $\tilde{a}_1^2 < -4\tilde{a}_3$ and $\tilde{a}_3 < 0$. The local phase portrait at the saddle-focus/center point of system (10) is shown in Figure 6.

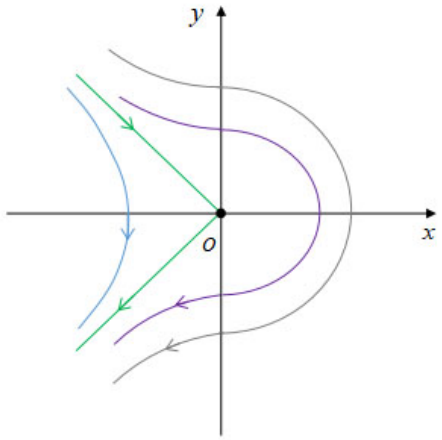

Figure 6. Local phase portrait at the saddle-focus/center point of system (10).

Proof. From $D_1 < 0$, $D_2 > 0$ and $\Delta_2 < 0$ it follows that

$$a_2 \neq 0, \quad T_2 = a_1 + a_4 \in (-2\sqrt{D_2}, 2\sqrt{D_2}).$$

With the transformation $(y,t) \to (y + a_4/a_2 x, t/a_2)$, system (5) is changed into (10), where $\tilde{b}_1 = T_1/a_2$, $\tilde{b}_2 = -D_1/a_2^2$, $\tilde{a}_1 = T_2/a_2 \in (-2\sqrt{D_2}/a_2, 2\sqrt{D_2}/a_2)$ and $\tilde{a}_2 = -D_2/a_2^2$. Thus, according to Theorem 1, we obtain the local phase portrait at the saddle-focus/center point of system (10) as shown in Figure 6. □

3.4. **Boundary-node point.** In this subsection, we discuss local phase portraits at the boundary-node point for system (5).

Theorem 6. *Suppose that $D_1 > 0$, $D_2 > 0$, $\Delta_1 \geq 0$ and $\Delta_2 \geq 0$ for system* (5)*. When $a_2 = 0$, system* (5) *is topologically equivalent to*

$$\dot{x} = \begin{cases} \tilde{b}_1 x, & \text{if } x < 0, \\ \tilde{a}_1 x, & \text{if } x > 0, \end{cases} \quad \dot{y} = \begin{cases} \tilde{b}_2 x + y, & \text{if } x < 0, \\ \tilde{a}_3 x + y, & \text{if } x > 0, \end{cases} \tag{11}$$

where $\tilde{b}_1 > 0$, $\tilde{b}_2 = 0$ if $\tilde{b}_1 \neq 1$, $\tilde{b}_2 \geq 0$ if $\tilde{b}_1 = 1$, $\tilde{a}_1 > 0$, $\tilde{a}_3 = 0$ if $\tilde{a}_1 \neq 1$ and $\tilde{a}_3 \in \mathbb{R}$ if $\tilde{a}_1 = 1$, see Table 1. Local phase portraits at the boundary-node points of system (11) *are presented in* Figure 7*.*

When $a_2 > 0$, system (5) *is topologically equivalent to*

$$\dot{x} = \begin{cases} \tilde{b}_1 x + y, & \text{if } x < 0, \\ \tilde{a}_1 x + y, & \text{if } x > 0, \end{cases} \quad \dot{y} = \begin{cases} \tilde{b}_2 x, & \text{if } x < 0, \\ \tilde{a}_3 x, & \text{if } x > 0, \end{cases} \tag{12}$$

where $\tilde{b}_1 \geq 2\sqrt{-\tilde{b}_2}$, $\tilde{b}_2 < 0$, $\tilde{a}_1^2 \geq -4\tilde{a}_3$ and $\tilde{a}_3 < 0$. Local phase portraits at the boundary-node points of system (12) *are shown in* Figure 8*.*

Table 1. Cases of boundary-node points

Cases of parameters of system (5)		Cases of parameters of system (11)	
In the $\mathcal{S}_l$	In the $\mathcal{S}_r$	In the $\mathcal{S}_l$	In the $\mathcal{S}_r$
$b_1 = a_4$, $b_2 = 0$	$a_1 = a_4$, $a_3 \neq 0$	$\tilde{b}_1 = 1$, $\tilde{b}_2 = 0$	$\tilde{a}_1 = 1$, $\tilde{a}_3 = \frac{a_3}{a_4} > 0$
	$\lvert a_1\rvert > \lvert a_4\rvert$		$\tilde{a}_1 = \frac{a_1}{a_4} > 1$, $\tilde{a}_3 = 0$
	$\lvert a_1\rvert < \lvert a_4\rvert$		$\tilde{a}_1 = \frac{a_1}{a_4} \in (0,1)$, $\tilde{a}_3 = 0$
$b_1 = a_4$, $b_2 \neq 0$	$a_1 = a_4$, $a_3 \neq 0$	$\tilde{b}_1 = 1$, $\tilde{b}_2 = \frac{b_2}{a_4} > 0$	$\tilde{a}_1 = 1$, $\tilde{a}_3 = \frac{a_3}{a_4} \neq 0$
	$\lvert a_1\rvert > \lvert a_4\rvert$		$\tilde{a}_1 = \frac{a_1}{a_4} > 1$, $\tilde{a}_3 = 0$
	$\lvert a_1\rvert < \lvert a_4\rvert$		$\tilde{a}_1 = \frac{a_1}{a_4} \in (0,1)$, $\tilde{a}_3 = 0$
$\lvert b_1\rvert > \lvert a_4\rvert$	$\lvert a_1\rvert > \lvert a_4\rvert$	$\tilde{b}_1 = \frac{b_1}{a_4} > 1$, $\tilde{b}_2 = 0$	$\tilde{a}_1 = \frac{a_1}{a_4} > 1$, $\tilde{a}_3 = 0$
	$\lvert a_1\rvert < \lvert a_4\rvert$		$\tilde{a}_1 = \frac{a_1}{a_4} \in (0,1)$, $\tilde{a}_3 = 0$
$\lvert b_1\rvert < \lvert a_4\rvert$	$\lvert a_1\rvert < \lvert a_4\rvert$	$\tilde{b}_1 = \frac{b_1}{a_4} \in (0,1)$, $\tilde{b}_2 = 0$	$\tilde{a}_1 = \frac{a_1}{a_4} \in (0,1)$, $\tilde{a}_3 = 0$

Proof. When $a_2 = 0$, from $D_1 > 0$ and $D_2 > 0$ it follows that

$$a_1 a_4 > 0, \quad b_1 a_4 > 0.$$

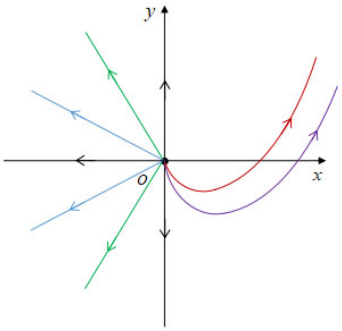

(a) $\tilde{b}_1 = 1$, $\tilde{b}_2 = 0$, $\tilde{a}_1 = 1$, $\tilde{a}_3 > 0$

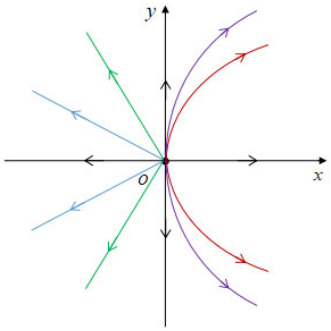

(b) $\tilde{b}_1 = 1$, $\tilde{b}_2 = 0$, $\tilde{a}_1 > 1$, $\tilde{a}_3 = 0$

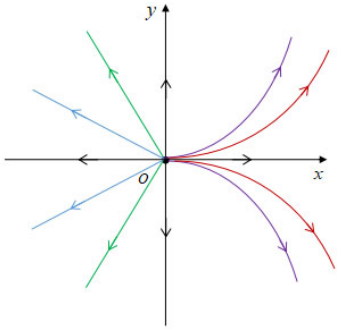

(c) $\tilde{b}_1 = 1$, $\tilde{b}_2 = 0$, $\tilde{a}_1 \in (0,1)$, $\tilde{a}_3 = 0$

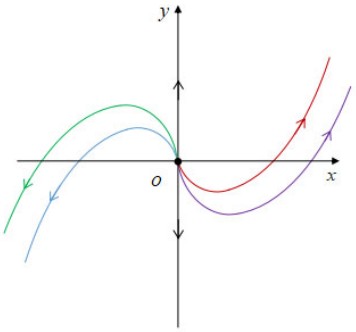

(d) $\tilde{b}_1 = 1$, $\tilde{b}_2 > 0$, $\tilde{a}_1 = 1$, $\tilde{a}_3 > 0$

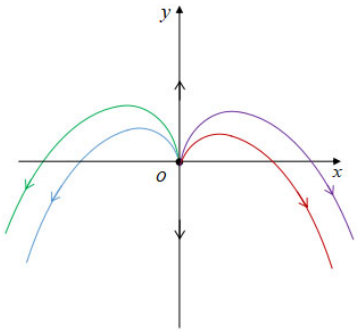

(e) $\tilde{b}_1 = 1$, $\tilde{b}_2 > 0$, $\tilde{a}_1 = 1$, $\tilde{a}_3 < 0$

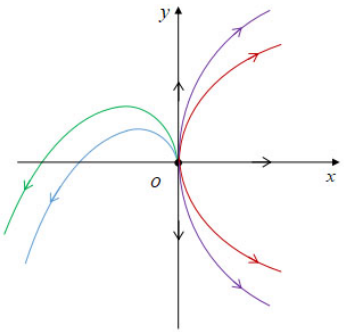

(f) $\tilde{b}_1 = 1$, $\tilde{b}_2 > 0$, $\tilde{a}_1 > 1$, $\tilde{a}_3 = 0$

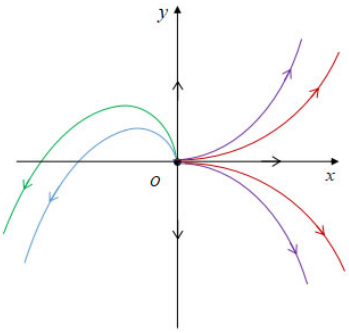

(g) $\tilde{b}_1 = 1$, $\tilde{b}_2 > 0$, $\tilde{a}_1 \in (0,1)$, $\tilde{a}_3 = 0$

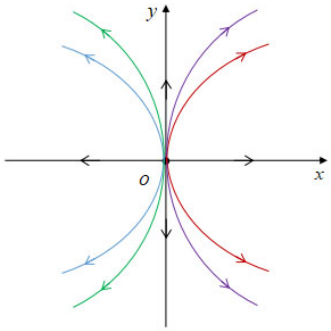

(h) $\tilde{b}_1 > 1$, $\tilde{b}_2 = 0$, $\tilde{a}_1 > 1$, $\tilde{a}_3 = 0$

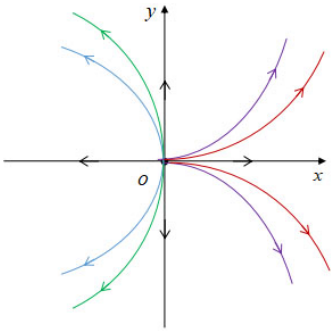

(i) $\tilde{b}_1 > 1$, $\tilde{b}_2 = 0$, $\tilde{a}_1 \in (0,1)$, $\tilde{a}_3 = 0$

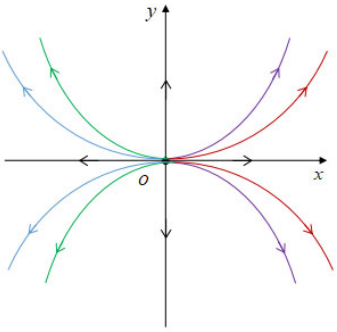

(j) $\tilde{b}_1 \in (0,1)$, $\tilde{b}_2 = 0$, $\tilde{a}_1 \in (0,1)$, $\tilde{a}_3 = 0$

Figure 7. Local phase portraits of the boundary-node points of system (11).

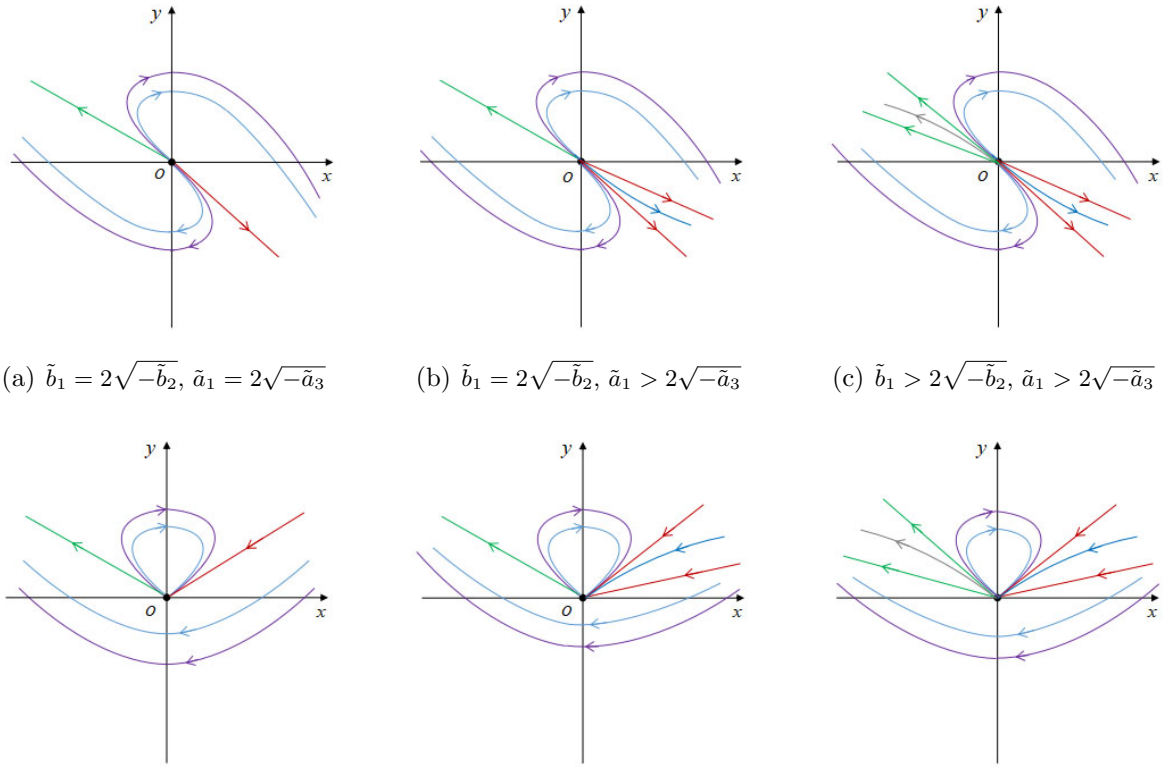

(a) $\tilde{b}_1 = 2\sqrt{-\tilde{b}_2},\ \tilde{a}_1 = 2\sqrt{-\tilde{a}_3}$ (b) $\tilde{b}_1 = 2\sqrt{-\tilde{b}_2},\ \tilde{a}_1 > 2\sqrt{-\tilde{a}_3}$ (c) $\tilde{b}_1 > 2\sqrt{-\tilde{b}_2},\ \tilde{a}_1 > 2\sqrt{-\tilde{a}_3}$

(d) $\tilde{b}_1 = 2\sqrt{-\tilde{b}_2},\ \tilde{a}_1 = -2\sqrt{-\tilde{a}_3}$ (e) $\tilde{b}_1 = 2\sqrt{-\tilde{b}_2},\ \tilde{a}_1 < -2\sqrt{-\tilde{a}_3}$ (f) $\tilde{b}_1 > 2\sqrt{-\tilde{b}_2},\ \tilde{a}_1 < -2\sqrt{-\tilde{a}_3}$

Figure 8. Local phase portraits of the boundary-node points of system (12).

In the zone $\mathcal{S}_l$, when $b_1 = a_4$, with a scaling $t \to t/a_4$, system (5) is changed into (11), where $\tilde{b}_1 = 1$ and $\tilde{b}_2 = b_2/a_4$. When $b_1 \neq a_4$, with the transformation

$$(y, t) \to \left(y + \frac{b_2}{b_1 - a_4} x,\ \frac{t}{a_4} \right),$$

system (5) is changed into (11), where $\tilde{b}_1 = b_1/a_4 \in (0, 1) \cup (1, +\infty)$ and $\tilde{b}_2 = 0$. It is easy to see that $\tilde{b}_1 > 1$ for $|b_1| > |a_4|$ and $\tilde{b}_1 \in (0, 1)$ for $|b_1| < |a_4|$. When $a_1 = a_4$ or $a_1 \neq a_4$, it reduces to system (11) in the zone $\mathcal{S}_r$, see Table 1. Note that system (11) is invariant under the transformation $(y, \tilde{b}_2, \tilde{a}_3) \to -(y, \tilde{b}_2, \tilde{a}_3)$ when $\tilde{b}_1 = 1, \tilde{b}_2 = b_2/a_4 \neq 0, \tilde{a}_1 > 0$ and $\tilde{a}_3 \in \mathbb{R}$. Thus, we only need to consider the positive case for $\tilde{b}_2$. Since system (11) is invariant under the transformation $(y, \tilde{a}_3) \to (-y, -\tilde{a}_3)$ when $\tilde{b}_1 = 1, \tilde{b}_2 = 0, \tilde{a}_1 = 1$ and $\tilde{a}_3 = a_3/a_4 \neq 0$, we only need to consider the positive case for $\tilde{a}_3$.

When $a_2 > 0$, from $D_1 > 0$, $D_2 > 0$, $\Delta_1 \geq 0$ and $\Delta_2 \geq 0$ it follows that

$$\begin{aligned} &a_2 \neq 0, T_1 = b_1 + a_4 \in (-\infty, -2\sqrt{D_1}] \cup [2\sqrt{D_1}, +\infty), \\ &T_2 = a_1 + a_4 \in (-\infty, -2\sqrt{D_2}] \cup [2\sqrt{D_2}, +\infty). \end{aligned}$$

With the transformation $(y, t) \to (y + a_4/a_2 x, t/a_2)$, system (5) reduces to (12), where

$$\begin{aligned} &\tilde{b}_1 = T_1/a_2 \in (-\infty, -2\sqrt{D_1}/a_2] \cup [2\sqrt{D_1}/a_2, +\infty), \tilde{b}_2 = -D_1/a_2^2, \\ &\tilde{a}_1 = T_2/a_2 \in (-\infty, -2\sqrt{D_2}/a_2] \cup [2\sqrt{D_2}/a_2, +\infty), \tilde{a}_3 = -D_2/a_2^2. \end{aligned}$$

Note that system (12) is invariant under the transformation $(y,t,\tilde{b}_1,\tilde{a}_1)\to-(y,t,\tilde{b}_1,\tilde{a}_1)$. Hence, we only need to consider the case $\tilde{b}_1\in[2\sqrt{D_1}/a_2,+\infty)$, i.e., $\tilde{b}_1\geq 2\sqrt{-\tilde{b}_2}$.

Using Theorem 1, we can obtain local phase portraits at the boundary-node point of system systems (11) as shown in Figure 7 and local phase portraits at the boundary-node points of system (12) as shown in Figure 8. □

3.5. **Node-focus point.** In this subsection we present local phase portraits at the node-focus points for system (5).

Theorem 7. *Suppose that $D_1>0$, $D_2>0$, $\Delta_1\geq 0$ and $\Delta_2<0$ for system (5). Then for $T_1>0$ system (5) is topologically equivalent to*

$$\dot{x}=\begin{cases}\tilde{b}_1x+y, & \text{if } x<0,\\ \tilde{a}_1x+y, & \text{if } x>0,\end{cases}\qquad \dot{y}=\begin{cases}\tilde{b}_2x, & \text{if } x<0,\\ \tilde{a}_3x, & \text{if } x>0,\end{cases}\tag{13}$$

where $\tilde{b}_1\geq 2\sqrt{-\tilde{b}_2}$, $\tilde{b}_2<0$, $\tilde{a}_1^2<-4\tilde{a}_3$ and $\tilde{a}_3<0$. Local phase portraits at the node-focus/center points of system (13) are shown in Figure 9.

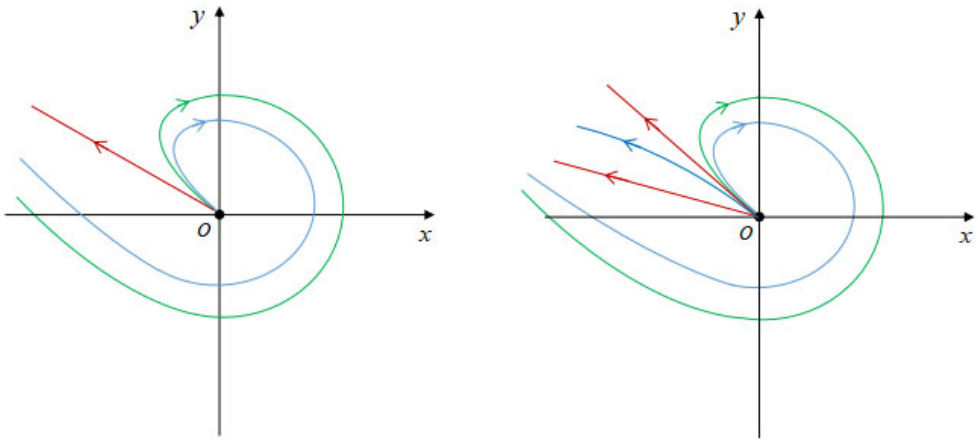

(a) $\tilde{b}_1=2\sqrt{-\tilde{b}_2}$ (b) $\tilde{b}_1>2\sqrt{-\tilde{b}_2}$

Figure 9. Local phase portraits at the node-focus/center point of system (13).

Due to $D_1>0$ and $\Delta_1\geq 0$, we get

$$T_1\in(-\infty,-2\sqrt{D_1}]\cup[2\sqrt{D_1},+\infty).$$

Note that system (13) is invariant under the transformation $(y,t,\tilde{b}_1,\tilde{a}_1)\to-(y,t,\tilde{b}_1,\tilde{a}_1)$. Hence, we only need to consider the case $T_1>0$ in Theorem 7.

Proof. From $D_1>0$, $D_2>0$, $\Delta_1\geq 0$, $\Delta_2<0$ and $T_1>0$, it follows that

$$a_2\neq 0,\ T_1=b_1+a_4\in[2\sqrt{D_1},+\infty),\ T_2=a_1+a_4\in(-2\sqrt{D_2},2\sqrt{D_2}).$$

With the transformation $(y,t)\to(y+a_4/a_2x,t/a_2)$, system (5) is changed into (13), where

$$\begin{aligned}&\tilde{b}_1=T_1/a_2\in[2\sqrt{D_1}/a_2,+\infty),\quad \tilde{b}_2=-D_1/a_2^2,\\ &\tilde{a}_1=T_2/a_2\in(-2\sqrt{D_2}/a_2,2\sqrt{D_2}/a_2),\quad \tilde{a}_2=-D_2/a_2^2.\end{aligned}$$

Thus, according to Theorem 1 we can obtain local phase portraits at the node-focus points of system (13) as shown in Figure 9. □

3.6. **Boundary-focus point and boundary-center point.** In this subsection, we discuss local phase portraits at the boundary-focus points and boundary-center points for system (5).

Theorem 8. *Suppose that $D_1 > 0$, $D_2 > 0$, $\Delta_1 < 0$ and $\Delta_2 < 0$ for system (5). Then system (5) is topologically equivalent to*

$$\dot{x} = \begin{cases} \tilde{b}_1 x + y, & \text{if } x < 0, \\ \tilde{a}_1 x + y, & \text{if } x > 0, \end{cases} \quad \dot{y} = \begin{cases} \tilde{b}_2 x, & \text{if } x < 0, \\ \tilde{a}_3 x, & \text{if } x > 0, \end{cases} \tag{14}$$

where $\tilde{b}_1^2 < -4\tilde{b}_2$, $\tilde{b}_2 < 0$, $\tilde{a}_1^2 < -4\tilde{a}_3$ and $\tilde{a}_3 < 0$. The origin O is a stable boundary-focus when $\tilde{b}_1/\sqrt{-\tilde{b}_2} + \tilde{a}_1/\sqrt{-\tilde{a}_3} > 0$, a boundary-center when $\tilde{b}_1/\sqrt{-\tilde{b}_2} + \tilde{a}_1/\sqrt{-\tilde{a}_3} = 0$, and an unstable boundary-focus when $\tilde{b}_1/\sqrt{-\tilde{b}_2} + \tilde{a}_1/\sqrt{-\tilde{a}_3} < 0$, see Figure 10.

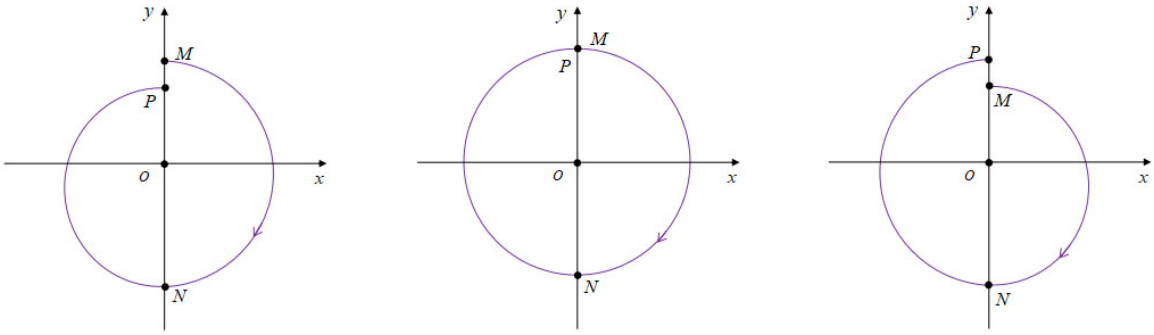

(a) $\tilde{b}_1/\sqrt{-\tilde{b}_2} + \tilde{a}_1/\sqrt{-\tilde{a}_3} > 0$ (b) $\tilde{b}_1/\sqrt{-\tilde{b}_2} + \tilde{a}_1/\sqrt{-\tilde{a}_3} = 0$ (c) $\tilde{b}_1/\sqrt{-\tilde{b}_2} + \tilde{a}_1/\sqrt{-\tilde{a}_3} < 0$

Figure 10. Local phase portraits at the boundary-focus/center point of system (14).

Proof. From $D_1 > 0$, $D_2 > 0$, $\Delta_1 < 0$ and $\Delta_2 < 0$, it follows that

$$a_2 \neq 0,\ T_1 = b_1 + a_4 \in (-2\sqrt{D_1}, 2\sqrt{D_1}),\ T_2 = a_1 + a_4 \in (-2\sqrt{D_2}, 2\sqrt{D_2}).$$

When $a_2 > 0$, with the transformation $(y, t) \to (y + a_4/a_2 x, t/a_2)$, system (5) reduces to (14), where

$$\begin{aligned} \tilde{b}_1 &= T_1/a_2 \in (-2\sqrt{D_1}/a_2, 2\sqrt{D_1}/a_2), \quad \tilde{b}_2 = -D_1/a_2^2, \\ \tilde{a}_1 &= T_2/a_2 \in (-2\sqrt{D_2}/a_2, 2\sqrt{D_2}/a_2), \quad \tilde{a}_3 = -D_2/a_2^2. \end{aligned}$$

With the transformation

$$(x, y) \to \left(-\sqrt{\frac{\tilde{a}_3}{\tilde{b}_2}} x, y \right)$$

in the zone $\mathcal{S}_l$, system (14) can be rewritten as

$$\frac{dy}{dx} = \frac{\tilde{a}_3 x}{y - \tilde{b}_1 \sqrt{\frac{\tilde{a}_3}{\tilde{b}_2}} x}. \tag{15}$$

In the zone $\mathcal{S}_r$, systems (14) becomes

$$\frac{dy}{dx} = \frac{\tilde{a}_3 x}{y + \tilde{a}_1 x}. \tag{16}$$

To characterize the stability of equilibrium O of system (14), we let $M(0, y_M)$ be a point on the positive y-axis in $\mathcal{D}_1$ with a small $|y_M|$ and $\varphi(M, I^+)$ be the positive orbit of system (14) with the initial point M. Since $\tilde{b}_2, \tilde{a}_3 < 0$, $\tilde{b}_1^2 + 4\tilde{b}_2 < 0$ and $\tilde{a}_1 + 4\tilde{a}_3 < 0$, the solution orbit $\varphi(M, I^+)$ of system (14) passing through M must intersect the positive and negative y-axis at $P(0, y_P)$ and $N(0, y_N)$ respectively, with $y_N < 0$ and $y_P > 0$.

When $\tilde{b}_1/\sqrt{-\tilde{b}_2} + \tilde{a}_1/\sqrt{-\tilde{a}_3} > 0$, we obtain

$$\frac{\tilde{a}_3 x}{y - \tilde{b}_1\sqrt{\frac{\tilde{a}_3}{\tilde{b}_2}}x} > \frac{\tilde{a}_3 x}{y + \tilde{a}_1 x}.$$

By the comparison theorem, the orbit arc of (15) connecting the point N from the point P is strictly located on the right side of the orbit arc connecting the point N from the point M of (16), i.e., $y_M > y_P > 0$. Thus, the equilibrium O of system (14) is a stable boundary-focus, as shown in Figure 10(a). Similarly, when $\tilde{b}_1/\sqrt{-\tilde{b}_2} + \tilde{a}_1/\sqrt{-\tilde{a}_3} = 0$, we deduce

$$\frac{\tilde{a}_3 x}{y - \tilde{b}_1\sqrt{\frac{\tilde{a}_3}{\tilde{b}_2}}x} \equiv \frac{\tilde{a}_3 x}{y + \tilde{a}_1 x}.$$

This indicates that $y_P \equiv y_M$ based on the theory of the existence and uniqueness of solutions of ordinary differential equations. Thus, the equilibrium O of system (14) is a boundary-center, as shown in Figure 10(b). When $\tilde{b}_1/\sqrt{-\tilde{b}_2} + \tilde{a}_1/\sqrt{-\tilde{a}_3} < 0$, we have

$$\frac{\tilde{a}_3 x}{y - \tilde{b}_1\sqrt{\frac{\tilde{a}_3}{\tilde{b}_2}}x} < \frac{\tilde{a}_3 x}{y + \tilde{a}_1 x}.$$

By the comparison theorem, the orbit arc of (15) connecting the point N from the point P is strictly located on the left side of the orbit arc connecting the point N from the point M of (16), i.e., $y_P > y_M > 0$. Thus, the equilibrium O of system (14) is an unstable boundary-focus, as shown in Figure 10(c). □

3.7. **Indices of boundary-equilibria.** The following proposition follows from [20, Section 6 of Chapter 2].

Proposition 9. [20, p.164] *Consider the system*

$$\frac{dx}{dt} = X(x, y), \quad \frac{dy}{dt} = Y(x, y), \tag{17}$$

where $X(x, y)$ and $Y(x, y)$ are continuous functions in a sufficiently small neighborhood $S_\delta(O)$ of the origin O. Moreover, let O be a boundary-equilibrium of system (17)*. Let e and p be the numbers of elliptic and parabolic sectors respectively, and h be the sum of the hyperbolic and hyperbolic-elliptic sectors. Suppose that I_O is the index of the equilibrium O. Then we have*

$$I_O = 1 + \frac{e - h}{2}.$$

Taking into account Proposition 9, we can obtain the following result.

Theorem 10. *For system* (5)*, when the origin is a boundary-saddle, we have the index* $I_O = -1$*. When the origin is a saddle-node or a saddle-focus, we have the index* $I_O = 0$*. When the origin is a boundary-node, or a boundary-focus, or a boundary-center, or a node-focus, we have the index* $I_O = 1$*.*

Proof. Firstly, we present the qualitative property of the origin O of system (5) in Table 2. For simplicity, we do not consider the number of parabolic sector p. By virtue of Proposition 9 and Table 2, when the origin is a boundary-saddle, we have $h = 4$ and $e = 0$, which leads to $I_O = 1 + (e - h)/2 = -1$. When the origin is a saddle-node or a saddle-focus, we have $h = 2$ and $e = 0$, which leads to $I_O = 1 + (e - h)/2 = 0$. When the origin is a boundary-node, or a boundary-focus, or a boundary-center, or a node-focus, we have $h = e = 0$, which gives $I_O = 1 + (e - h)/2 = 1$. □

4. Phase portraits and indices of singular continuum

In this section, we study phase portraits and indices of singular continuums for continuous piecewise linear systems.

We consider a local region $\mathcal{D}_2 \subset \mathbb{R}^2$ of phase space that just contains one singular continuum and the origin. Without loss of generality, continuous piecewise linear systems in region $\mathcal{D}_2$ can be transformed to

$$
\begin{aligned}
\dot{x} &= \begin{cases} b_1 x + a_2 y, & \text{if } x < 0, \\ -a_2 y_0 x/x_0 + a_2 y, & \text{if } 0 < x < x_0, \\ a_1(x - x_0) + a_2(y - y_0), & \text{if } x > x_0, \end{cases} \\
\dot{y} &= \begin{cases} b_2 x + a_4 y, & \text{if } x < 0, \\ -a_4 y_0 x/x_0 + a_4 y, & \text{if } 0 < x < x_0, \\ a_3(x - x_0) + a_4(y - y_0), & \text{if } x > x_0, \end{cases}
\end{aligned} \tag{18}
$$

where $(a_1, a_2, a_3, a_4, b_1, b_2, y_0) \in \mathbb{R}^7$, $(x, y) \in \mathcal{D}_2$, $a_4 b_1 - a_2 b_2 \neq 0$ and $a_1 a_4 - a_2 a_3 \neq 0$. We call the continuum of non-isolated equilibria $\omega = \{(x, y) \in \mathcal{D}_2 : y = y_0 x/x_0, 0 \leq x \leq x_0\}$ of system (18) to be a singular continuum. For system (18), we assume $a_2 \geq 0$. If $a_2 < 0$, the argument can be processed similarly by a transform $y \to -y$.

For system (18), the switching lines $x = 0$ and $x = x_0$ separate $\mathcal{D}_2$ into five regions as follows:

$$
\begin{aligned}
&\mathcal{S}_L := \{(x, y) \in \mathcal{D}_2 : x < 0\}, \quad \mathcal{S}_C := \{(x, y) \in \mathcal{D}_2 : 0 < x < x_0\}, \\
&\mathcal{S}_R := \{(x, y) \in \mathcal{D}_2 : x > x_0\}, \\
&\Sigma_{C_1} := \{(x, y) \in \mathcal{D}_2 : x = 0\}, \quad \Sigma_{C_2} := \{(x, y) \in \mathcal{D}_2 : x = x_0\},
\end{aligned}
$$

where $\mathcal{D}_2 := \mathcal{S}_L \cup \mathcal{S}_C \cup \mathcal{S}_R \cup \Sigma_{C_1} \cup \Sigma_{C_2}$. The Jacobian matrices in the $\mathcal{S}_L$, $\mathcal{S}_C$ and $\mathcal{S}_R$ are

$$
J_L := \begin{pmatrix} b_1 & a_2 \\ b_2 & a_4 \end{pmatrix}, \quad J_C := \begin{pmatrix} -a_2 y_0/x_0 & a_2 \\ -a_4 y_0/x_0 & a_4 \end{pmatrix}, \quad J_R := \begin{pmatrix} a_1 & a_2 \\ a_3 & a_4 \end{pmatrix},
$$

respectively. Then we have

$$
\begin{aligned}
&D_1 := \det J_L = a_4 b_1 - a_2 b_2, \quad D_2 := \det J_R = a_1 a_4 - a_2 a_3, \quad D_3 := \det J_C = 0, \\
&T_1 := \mathrm{tr} J_L = a_4 + b_1, T_2 := \mathrm{tr} J_R = a_1 + a_4, \quad T_3 := \mathrm{tr} J_C = -a_2 y_0/x_0 + a_4, \\
&\Delta_1 := {T_1}^2 - 4D_1, \ \Delta_2 := {T_2}^2 - 4D_2.
\end{aligned}
$$

Table 2. Qualitative properties of O of system (5).

Type of O	Geometric configurations in $S_\delta(O)$
boundary-saddle	$h = 4$, $e = 0$, see Figures 2 and 3.
saddle-node	$h = 2$, $e = 0$, see Figures 4 and 5
saddle-focus/center	$h = 2$, $e = 0$, see Figure 6
boundary-node	When $\tilde{a}_1\tilde{b}_1 > 0$, then $h = 0$, $e = 0$, see Figures 7 and 8(a)-(c). When $\tilde{a}_1\tilde{b}_1 < 0$, then $h = 1$, $e = 1$, see Figure 8(d)-(f).
node-focus/center	$h = 0$, $e = 0$, see Figure 9
boundary-focus/center	$h = 0$, $e = 0$, see Figure 10

Consider the system

$$\begin{cases} \dot{x} = -a_2 y_0 x/x_0 + a_2 y, \\ \dot{y} = -a_4 y_0 x/x_0 + a_4 y, \end{cases} \tag{19}$$

where $0 \le x \le x_0$ and $x_0 > 0$.

Lemma 11. *When $a_2 = 0$, system (19) is topologically equivalent to*

$$\dot{x} = 0, \quad \dot{y} = -\tilde{c}_2 x + y, \tag{20}$$

where $0 \le x \le x_0$ and $\tilde{c}_2 \in \mathbb{R}$. Phase portraits in the strip $0 \le x \le x_0$ are shown in Figure 11. *When $a_2 > 0$, system (19) is topologically equivalent to*

$$\dot{x} = -\tilde{c}_1 x + y, \quad \dot{y} = 0, \tag{21}$$

where $0 \le x \le x_0$ and $\tilde{c}_1 \in \mathbb{R}$. Phase portraits in the strip $0 \le x \le x_0$ are shown in Figure 12.

Proof. When $a_2 = 0$, by a scaling $t \to t/a_4$, system (19) reduces to (20), where $\tilde{c}_2 = y_0/x_0$. When $a_2 > 0$, we use the transformation $(y, t) \to (y + a_4/a_2 x, t/a_2)$ to change system (19) to (21), where $\tilde{c}_1 = -T_3/a_2$. Consequently, we can derive phase diagrams of systems (20) and (21) in the strip $0 \le x \le x_0$ as shown in Figures 11 and 12, respectively. □

We call dynamical behavior of system (18) at $\mathcal{S}_L$ (resp. $\mathcal{S}_R$) is saddle type when $D_1 < 0$ (resp. $D_2 < 0$), node type when $D_1 > 0$ and $\Delta_1 \ge 0$ (resp. $D_2 > 0$ and $\Delta_2 \ge 0$), focus type when $T_1 \ne 0$, $D_1 > 0$ and $\Delta_1 < 0$ (resp. $T_2 \ne 0$, $D_2 > 0$ and $\Delta_2 < 0$), and center type when $D_1 > 0$ and $T_1 = 0$ (resp. $D_2 > 0$ and $T_2 = 0$). We say the singular continuum of system (18) to be a saddle-saddle continuum (resp. node-node continuum) if system (18) at $\mathcal{S}_L$ and $\mathcal{S}_R$ is saddle (resp., node). Moreover, we say the singular continuum of system

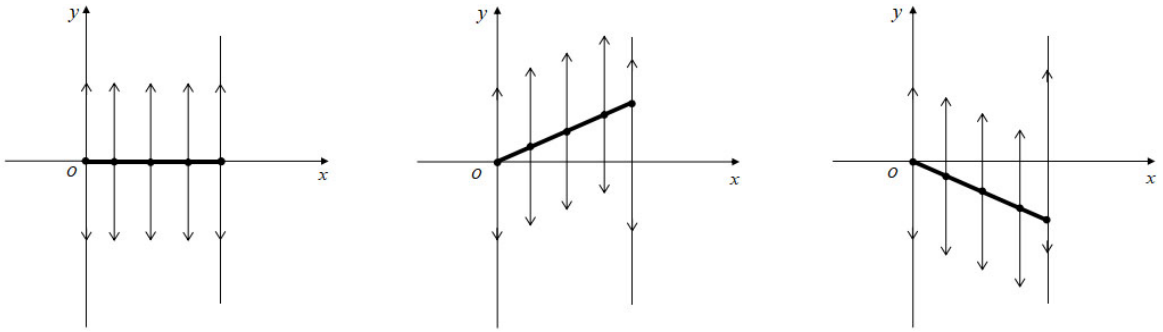

(a) $\tilde{c}_2 = 0$ (b) $\tilde{c}_2 > 0$ (c) $\tilde{c}_2 < 0$

Figure 11. Phase portraits of system (20) in the strip $0 \le x \le x_0$

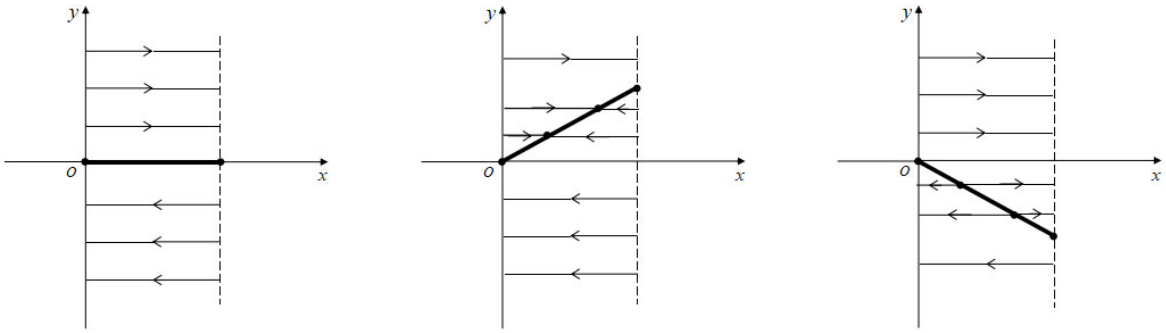

(a) $\tilde{c}_1 = 0$ (b) $\tilde{c}_1 > 0$ (c) $\tilde{c}_1 < 0$

Figure 12. Phase portraits of system (21) in the strip $0 \le x \le x_0$.

(18) to be a focus continuum (resp. center continuum) if all orbits tend toward the singular continuum (resp. all orbits form a family of closed curves around the singular continuum) spirally. We can define saddle-node continuum, saddle-focus continuum, saddle-center continuum, node-focus continuum and node-center continuum in a similar way.

4.1. **Saddle-saddle continuum.** We summarize local phase portraits at the saddle-saddle continuum for system (18) in the following theorem.

Theorem 12. *Suppose that* $D_1 < 0$ *and* $D_2 < 0$ *for system* (18). *When* $a_2 = 0$, *system* (18) *is topologically equivalent to*

$$\dot{x} = \begin{cases} \tilde{b}_1 x, & \text{if } x < 0, \\ 0, & \text{if } 0 < x < x_0, \\ \tilde{a}_1(x - x_0), & \text{if } x > x_0, \end{cases} \qquad \dot{y} = \begin{cases} y, & \text{if } x < 0, \\ -\tilde{c}_2 x + y, & \text{if } 0 < x < x_0, \\ y - \tilde{c}_2 x_0, & \text{if } x > x_0, \end{cases} \tag{22}$$

where $\tilde{b}_1 < 0$, $\tilde{a}_1 < 0$ *and* $\tilde{c}_2 \ge 0$. *Local phase portrait at the saddle-saddle continuum is shown in* Figure 13.

When $a_2 > 0$, system (18) *is topologically equivalent to*

$$(23)\quad \dot{x} = \begin{cases} \tilde{b}_1 x + y, & \text{if } x < 0, \\ -\tilde{c}_1 x + y, & \text{if } 0 < x < x_0, \\ \tilde{a}_1(x - x_0) + y - \tilde{c}_1 x_0, & \text{if } x > x_0, \end{cases} \quad \dot{y} = \begin{cases} \tilde{b}_2 x, & \text{if } x < 0, \\ 0, & \text{if } 0 < x < x_0, \\ \tilde{a}_3(x - x_0), & \text{if } x > x_0, \end{cases}$$

where $(\tilde{a}_1, \tilde{b}_1) \in \mathbb{R}^2$, $\tilde{a}_3$, $\tilde{b}_2 > 0$ *and* $\tilde{c}_1 \geq 0$. *Local phase portrait at the saddle-saddle continuum is shown in* Figure 14.

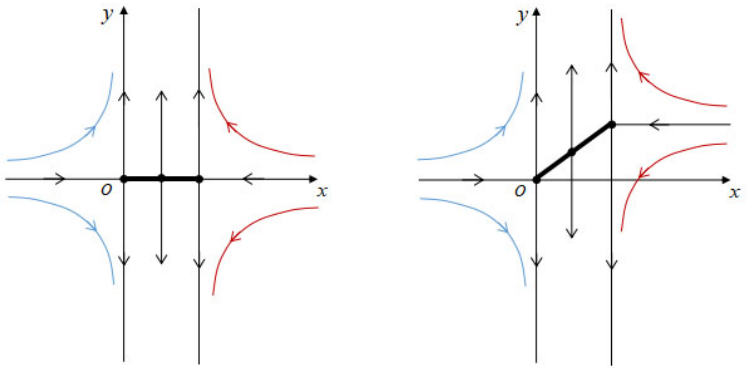

(a) $\tilde{c}_2 = 0$ (b) $\tilde{c}_2 > 0$

Figure 13. Local phase portrait at the saddle-saddle continuum of system (22).

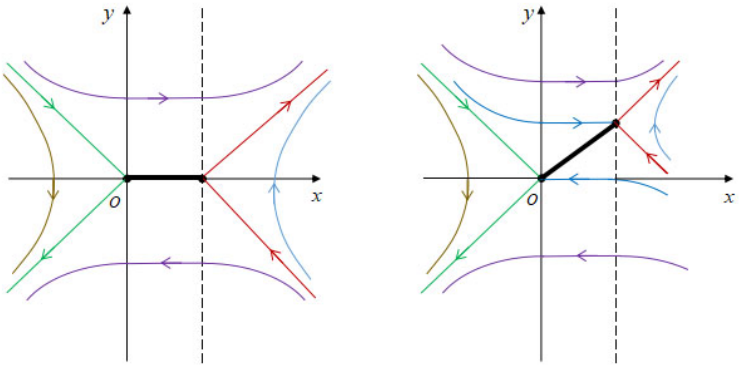

(a) $\tilde{c}_1 = 0$ (b) $\tilde{c}_1 > 0$

Figure 14. Local phase portrait at the saddle-saddle continuum of system (23).

Proof. By Theorem 3 and Lemma 11, it is easy to derive systems (22) and (23). For system (22), we have $\tilde{b}_1 = b_1/a_4 < 0$, $\tilde{a}_1 = a_1/a_4 < 0$ and $\tilde{c}_2 = y_0/x_0$. Since system (22) is invariant under the transformation $(y, \tilde{c}_2) \to (-y, -\tilde{c}_2)$, we only need to consider the case $\tilde{c}_2 \geq 0$. For system (23), we have

$$\tilde{b}_1 = T_1/a_2, \quad \tilde{b}_2 = -D_1/a_2^2, \quad \tilde{a}_1 = T_2/a_2, \quad \tilde{a}_2 = -D_2/a_2^2, \quad \tilde{c}_1 = -T_3/a_2.$$

Since system (23) is invariant by the transformation $(y, t, \tilde{a}_1, \tilde{b}_1, \tilde{c}_1) \to -(y, t, \tilde{a}_1, \tilde{b}_1, \tilde{c}_1)$, we only need to consider the case $\tilde{c}_1 \geq 0$. Thus, we can obtain the local phase portrait at the saddle-saddle continuum of system (22) as shown in Figure 13 and the local phase portrait at the saddle-saddle continuum of system (23) as shown in Figure 14. □

4.2. **Saddle-node continuum.** For local phase portrait at the saddle-node continuum for system (18), we have

Theorem 13. *Suppose that $D_1 < 0$, $D_2 > 0$ and $\Delta_2 \geq 0$ for system* (18)*. When $a_2 = 0$, system* (18) *is topologically equivalent to*

$$\dot{x} = \begin{cases} \tilde{b}_1 x, & \text{if } x < 0, \\ 0, & \text{if } 0 < x < x_0, \\ \tilde{a}_1(x - x_0), & \text{if } x > x_0, \end{cases} \quad \dot{y} = \begin{cases} y, & \text{if } x < 0, \\ -\tilde{c}_2 x + y, & \text{if } 0 < x < x_0, \\ \tilde{a}_3(x - x_0) + y - \tilde{c}_2 x_0, & \text{if } x > x_0, \end{cases} \tag{24}$$

where $\tilde{b}_1 < 0$, $\tilde{a}_1 > 0$, $\tilde{a}_3 = 0$ if $\tilde{a}_1 \neq 1$ and $\tilde{a}_3 \geq 0$ if $\tilde{a}_1 = 1$, and $\tilde{c}_2 \in \mathbb{R}$. Local phase portraits at the saddle-node continuum of system (24) *are shown in* Figure 15*.*

When $a_2 > 0$, system (18) *is topologically equivalent to*

$$\dot{x} = \begin{cases} \tilde{b}_1 x + y, & \text{if } x < 0, \\ -\tilde{c}_1 x + y, & \text{if } 0 < x < x_0, \\ \tilde{a}_1(x - x_0) + y - \tilde{c}_1 x_0, & \text{if } x > x_0, \end{cases} \quad \dot{y} = \begin{cases} \tilde{b}_2 x, & \text{if } x < 0, \\ 0, & \text{if } 0 < x < x_0, \\ \tilde{a}_3(x - x_0), & \text{if } x > x_0, \end{cases} \tag{25}$$

where $\tilde{b}_1 \in \mathbb{R}$, $\tilde{b}_2 > 0$, $\tilde{a}_1 \geq 2\sqrt{-\tilde{a}_3}$, $\tilde{a}_3 < 0$ and $\tilde{c}_1 \in \mathbb{R}$. Local phase portraits at the saddle-node continuum of system (25) *are shown in* Figure 16*.*

Proof. From Theorem 4 and Lemma 11, we can derive systems (24) and (25) immediately. For system (24), we have $\tilde{b}_1 = b_1/a_4 < 0$, $\tilde{a}_1 > 0$, $\tilde{a}_3 \geq 0$ and $\tilde{c}_2 = y_0/x_0$. Since system (24) is invariant under the transformation $(y, \tilde{c}_2) \to (-y, -\tilde{c}_2)$ when $\tilde{a}_3 = 0$, we only need to consider the case $\tilde{c}_2 \geq 0$. For system (25), we have $\tilde{b}_1 = T_1/a_2$, $\tilde{b}_2 = -D_1/a_2^2$, $\tilde{a}_1 = T_2/a_2 \in [2\sqrt{D_2}, +\infty)$, $\tilde{a}_3 = -D_2/a_2^2$ and $\tilde{c}_1 = -T_3/a_2$. Thus, we can obtain local phase portraits at the generalized saddle-node points of system (24) as shown in Figure 15 and local phase portraits at the saddle-node continuum of system (25) as shown in Figure 16. □

4.3. **Saddle-focus/center continuum.** In this subsection, we consider local phase portraits at the saddle-focus continuum for system (18).

Theorem 14. *Suppose that $D_1 < 0$, $D_2 > 0$ and $\Delta_2 < 0$ for system* (18)*. System* (18) *is topologically equivalent to*

$$\dot{x} = \begin{cases} \tilde{b}_1 x + y, & \text{if } x < 0, \\ -\tilde{c}_1 x + y, & \text{if } 0 < x < x_0, \\ \tilde{a}_1(x - x_0) + y - \tilde{c}_1 x_0, & \text{if } x > x_0, \end{cases} \quad \dot{y} = \begin{cases} \tilde{b}_2 x, & \text{if } x < 0, \\ 0, & \text{if } 0 < x < x_0, \\ \tilde{a}_3(x - x_0), & \text{if } x > x_0, \end{cases} \tag{26}$$

where $\tilde{b}_1 \in \mathbb{R}$, $\tilde{b}_2 > 0$, $\tilde{a}_1^2 < -4\tilde{a}_3$, $\tilde{a}_3 < 0$ and $\tilde{c}_1 \geq 0$. Local phase portraits at saddle-focus continuums of system (26) *are shown in* Figure 17*.*

Proof. By Theorem 5 and Lemma 11, we can derive system (26) immediately. For system (26), we have $\tilde{b}_1 = T_1/a_2$, $\tilde{b}_2 = -D_1/a_2^2$, $\tilde{a}_1 = T_2/a_2 \in (-2\sqrt{D_2}/a_2, 2\sqrt{D_2}/a_2)$, $\tilde{a}_3 = -D_2/a_2^2$ and $\tilde{c}_1 = -T_3/a_2$. Since system (26) is invariant under the transformation $(y, t, \tilde{a}_1, \tilde{b}_1, \tilde{c}_1) \to -(y, t, \tilde{a}_1, \tilde{b}_1, \tilde{c}_1)$, we only need to consider the case $\tilde{c}_1 \geq 0$. Thus, we can obtain local phase portraits at the saddle-focus continuum of system (26) as shown in Figure 17. □

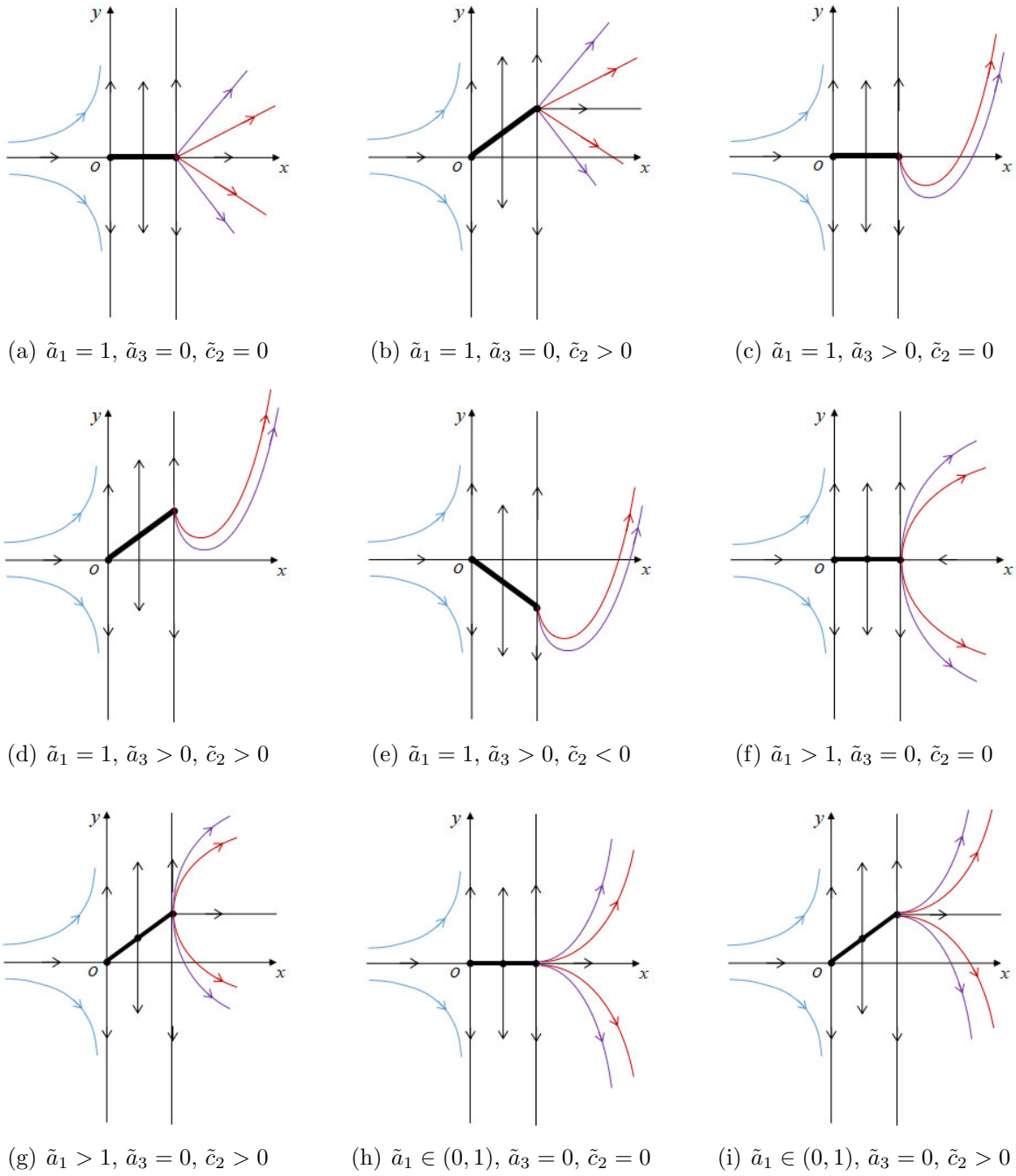

(a) $\tilde{a}_1 = 1$, $\tilde{a}_3 = 0$, $\tilde{c}_2 = 0$ (b) $\tilde{a}_1 = 1$, $\tilde{a}_3 = 0$, $\tilde{c}_2 > 0$ (c) $\tilde{a}_1 = 1$, $\tilde{a}_3 > 0$, $\tilde{c}_2 = 0$

(d) $\tilde{a}_1 = 1$, $\tilde{a}_3 > 0$, $\tilde{c}_2 > 0$ (e) $\tilde{a}_1 = 1$, $\tilde{a}_3 > 0$, $\tilde{c}_2 < 0$ (f) $\tilde{a}_1 > 1$, $\tilde{a}_3 = 0$, $\tilde{c}_2 = 0$

(g) $\tilde{a}_1 > 1$, $\tilde{a}_3 = 0$, $\tilde{c}_2 > 0$ (h) $\tilde{a}_1 \in (0,1)$, $\tilde{a}_3 = 0$, $\tilde{c}_2 = 0$ (i) $\tilde{a}_1 \in (0,1)$, $\tilde{a}_3 = 0$, $\tilde{c}_2 > 0$

Figure 15. Local phase portraits at the saddle-node continuum of system (24).

4.4. **Node-node continuum.** For local phase portraits at the node-node continuum for system (18), we have

Theorem 15. *Suppose that* $D_1 > 0$, $D_2 > 0$, $\Delta_1 \geq 0$ *and* $\Delta_2 \geq 0$ *for system* (18). *When* $a_2 = 0$, *system* (18) *is topologically equivalent to*

$$(27)\quad \dot{x} = \begin{cases} \tilde{b}_1 x, & \text{if } x < 0, \\ 0, & \text{if } 0 < x < x_0, \\ \tilde{a}_1(x - x_0), & \text{if } x > x_0, \end{cases} \quad \dot{y} = \begin{cases} \tilde{b}_2 x + y, & \text{if } x < 0, \\ -\tilde{c}_2 x + y, & \text{if } 0 < x < x_0, \\ \tilde{a}_3(x - x_0) + y - \tilde{c}_2 x_0, & \text{if } x > x_0, \end{cases}$$

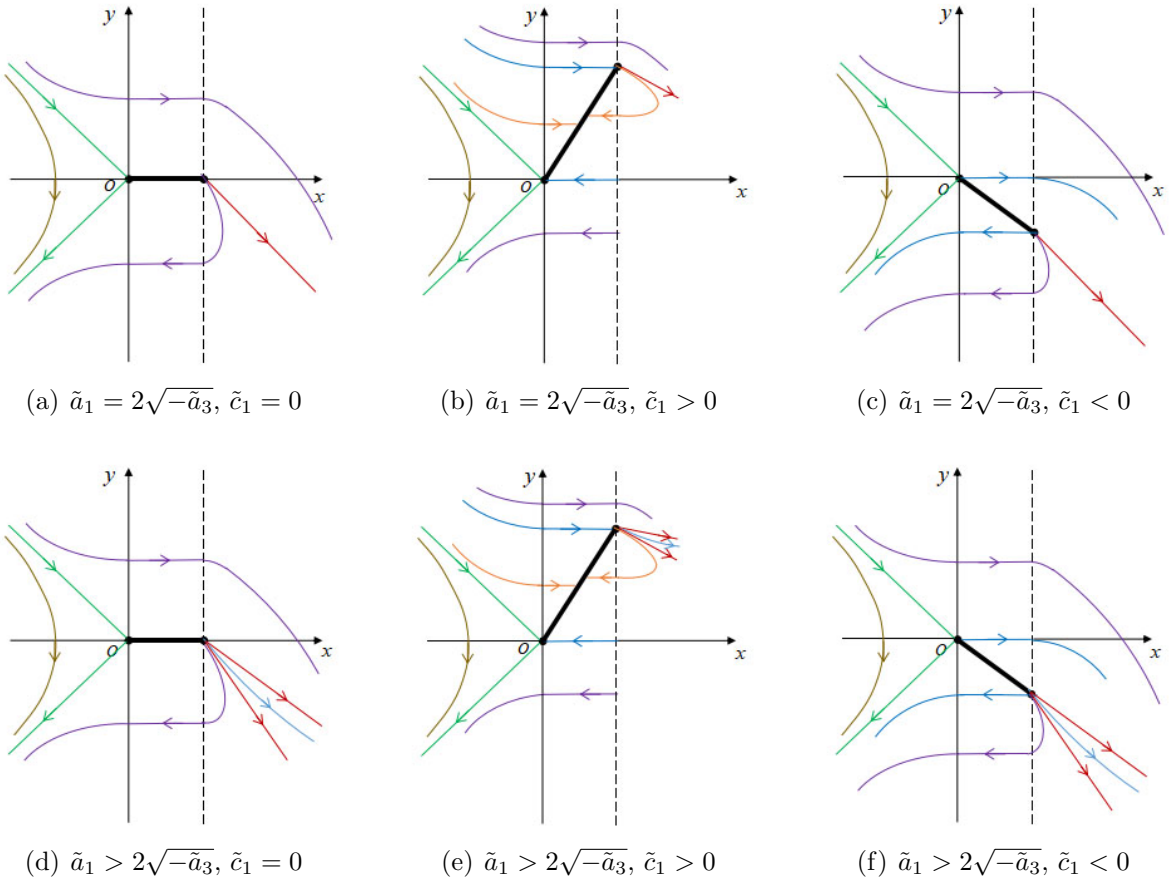

(a) $\tilde{a}_1 = 2\sqrt{-\tilde{a}_3}$, $\tilde{c}_1 = 0$ (b) $\tilde{a}_1 = 2\sqrt{-\tilde{a}_3}$, $\tilde{c}_1 > 0$ (c) $\tilde{a}_1 = 2\sqrt{-\tilde{a}_3}$, $\tilde{c}_1 < 0$

(d) $\tilde{a}_1 > 2\sqrt{-\tilde{a}_3}$, $\tilde{c}_1 = 0$ (e) $\tilde{a}_1 > 2\sqrt{-\tilde{a}_3}$, $\tilde{c}_1 > 0$ (f) $\tilde{a}_1 > 2\sqrt{-\tilde{a}_3}$, $\tilde{c}_1 < 0$

Figure 16. Local phase portraits at the saddle-node continuum of system (25).

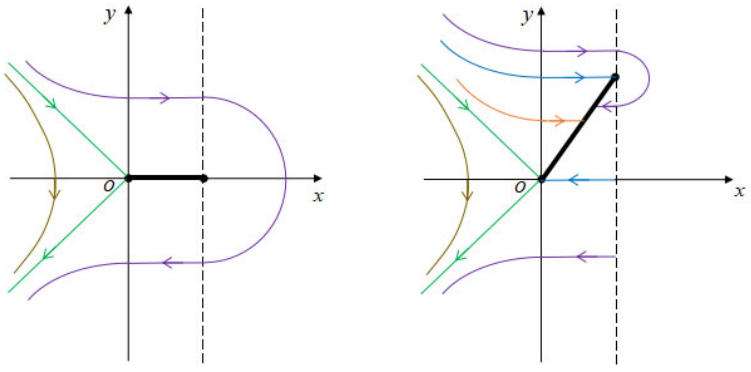

(a) $\tilde{c}_1 = 0$ (b) $\tilde{c}_1 > 0$

Figure 17. Local phase portraits at saddle-focus continuum of system (26).

where $\tilde{b}_1 > 0$, $\tilde{b}_2 = 0$ *if* $\tilde{b}_1 \neq 1$ *and* $\tilde{b}_2 \geq 0$ *if* $\tilde{b}_1 = 1$, $\tilde{a}_1 > 0$, $\tilde{a}_3 = 0$ *if* $\tilde{a}_1 \neq 1$ *and* $\tilde{a}_3 \in \mathbb{R}$ *if* $\tilde{a}_1 = 1$, *and* $\tilde{c}_2 \in \mathbb{R}$. *Local phase portraits at the node-node continuum of system* (27) *are shown in* Figures 18-20.

When $a_2 > 0$, system (18) *is topologically equivalent to*

$$(28)\quad \dot{x} = \begin{cases} \tilde{b}_1 x + y, & \text{if } x < 0, \\ -\tilde{c}_1 x + y, & \text{if } 0 < x < x_0, \\ \tilde{a}_1(x - x_0) + y - \tilde{c}_1 x_0, & \text{if } x > x_0, \end{cases} \quad \dot{y} = \begin{cases} \tilde{b}_2 x, & \text{if } x < 0, \\ 0, & \text{if } 0 < x < x_0, \\ \tilde{a}_3(x - x_0), & \text{if } x > x_0, \end{cases}$$

where $\tilde{b}_1 \geq 2\sqrt{-\tilde{b}_2}$, $\tilde{b}_2 < 0$, $\tilde{a}_1^2 \geq -4\tilde{a}_3$, $\tilde{a}_3 < 0$ and $\tilde{c}_1 \in \mathbb{R}$. Local phase portraits at the node-node continuum of system (28) *are shown in* Figures 21-22.

Proof. By Theorem 6 and Lemma 11, we can derive systems (27) and (28) respectively. For system (27), we have $\tilde{b}_1 = b_1/a_4 > 0$, $\tilde{b}_2 = b_2/a_4 \geq 0$, $\tilde{a}_1 = a_1/a_4 > 0$, $\tilde{a}_3 = a_3/a_4 \in \mathbb{R}$ and $\tilde{c}_2 = y_0/x_0 \in \mathbb{R}$. Since system (27) is invariant under the transformation $(y, \tilde{c}_2) \to (-y, -\tilde{c}_2)$ for $\tilde{b}_1 > 0$, $\tilde{b}_2 = 0$, $\tilde{a}_1 > 0$, and $\tilde{a}_3 = 0$, we only need to consider the case $\tilde{c}_2 \geq 0$. For system (28), we have $\tilde{b}_1 \geq 2\sqrt{-\tilde{b}_2}$, $\tilde{b}_2 < 0$, $\tilde{a}_1^2 \geq -4\tilde{a}_3$, $\tilde{a}_3 < 0$ and $\tilde{c}_1 = -T_3/a_2 \in \mathbb{R}$. Thus, we can obtain local phase portraits at the node-node continuum of system (27) as shown in Figures 18-20 and local phase portraits at the node-node continuum of system (28) as shown in Figures 21-22. □

4.5. **Node-focus continuum.** For local phase portraits at the node-focus continuum of system (18), we have

Theorem 16. *Suppose that $D_1 > 0$, $D_2 > 0$, $\Delta_1 \geq 0$ and $\Delta_2 < 0$ for system* (18)*. Then system* (18) *is topologically equivalent to*

$$(29)\quad \dot{x} = \begin{cases} \tilde{b}_1 x + y, & \text{if } x < 0, \\ -\tilde{c}_1 x + y, & \text{if } 0 < x < x_0, \\ \tilde{a}_1(x - x_0) + y - \tilde{c}_1 x_0, & \text{if } x > x_0, \end{cases} \quad \dot{y} = \begin{cases} \tilde{b}_2 x, & \text{if } x < 0, \\ 0, & \text{if } 0 < x < x_0, \\ \tilde{a}_3(x - x_0), & \text{if } x > x_0, \end{cases}$$

where $\tilde{b}_1 \geq 2\sqrt{-\tilde{b}_2}$, $\tilde{b}_2 < 0$, $\tilde{a}_1^2 < -4\tilde{a}_3$, $\tilde{a}_3 < 0$ and $\tilde{c}_1 \in \mathbb{R}$. Local phase portraits at the node-focus continuum of system (29) *are shown in* Figure 23.

The proof is closely analogous to that of Theorem 15, so we omit it.

4.6. **Focus continuum and center continuum.** For local phase portraits at the focus continuum and center continuum for system (18), we have

Theorem 17. *Suppose that $D_1 > 0$, $D_2 > 0$, $\Delta_1 < 0$ and $\Delta_2 < 0$ for system* (18)*. Then system* (18) *is topologically equivalent to*

$$(30)\quad \dot{x} = \begin{cases} \tilde{b}_1 x + y, & \text{if } x < 0, \\ -\tilde{c}_1 x + y, & \text{if } 0 < x < x_0, \\ \tilde{a}_1(x - x_0) + y - \tilde{c}_1 x_0, & \text{if } x > x_0, \end{cases} \quad \dot{y} = \begin{cases} \tilde{b}_2 x, & \text{if } x < 0, \\ 0, & \text{if } 0 < x < x_0, \\ \tilde{a}_3(x - x_0), & \text{if } x > x_0, \end{cases}$$

where $\tilde{b}_1^2 < -4\tilde{b}_2$, $\tilde{b}_2 < 0$, $\tilde{a}_1^2 < -4\tilde{a}_3$, $\tilde{a}_3 < 0$ and $\tilde{c}_1 \geq 0$. Local phase portraits at focus continuums and center continuums of system (30) *are shown in* Figure 24,

Proof. By Theorem 8 and Lemma 11, we can derive system (30) right away. For system (30), we have $\tilde{b}_1 = T_1/a_2 \in (-2\sqrt{D_1}/a_2, 2\sqrt{D_1}/a_2)$, $\tilde{b}_2 = -D_1/a_2^2$, $\tilde{a}_1 = T_2/a_2 \in (-2\sqrt{D_2}/a_2, 2\sqrt{D_2}/a_2)$, $\tilde{a}_3 = -D_2/a_2^2$ and $\tilde{c}_1 = -T_3/a_2$. Note that system (30) is invariant under the transformation $(y, t, \tilde{a}_1, \tilde{b}_1, \tilde{c}_1) \to -(y, t, \tilde{a}_1, \tilde{b}_1, \tilde{c}_1)$. Hence, we only need to

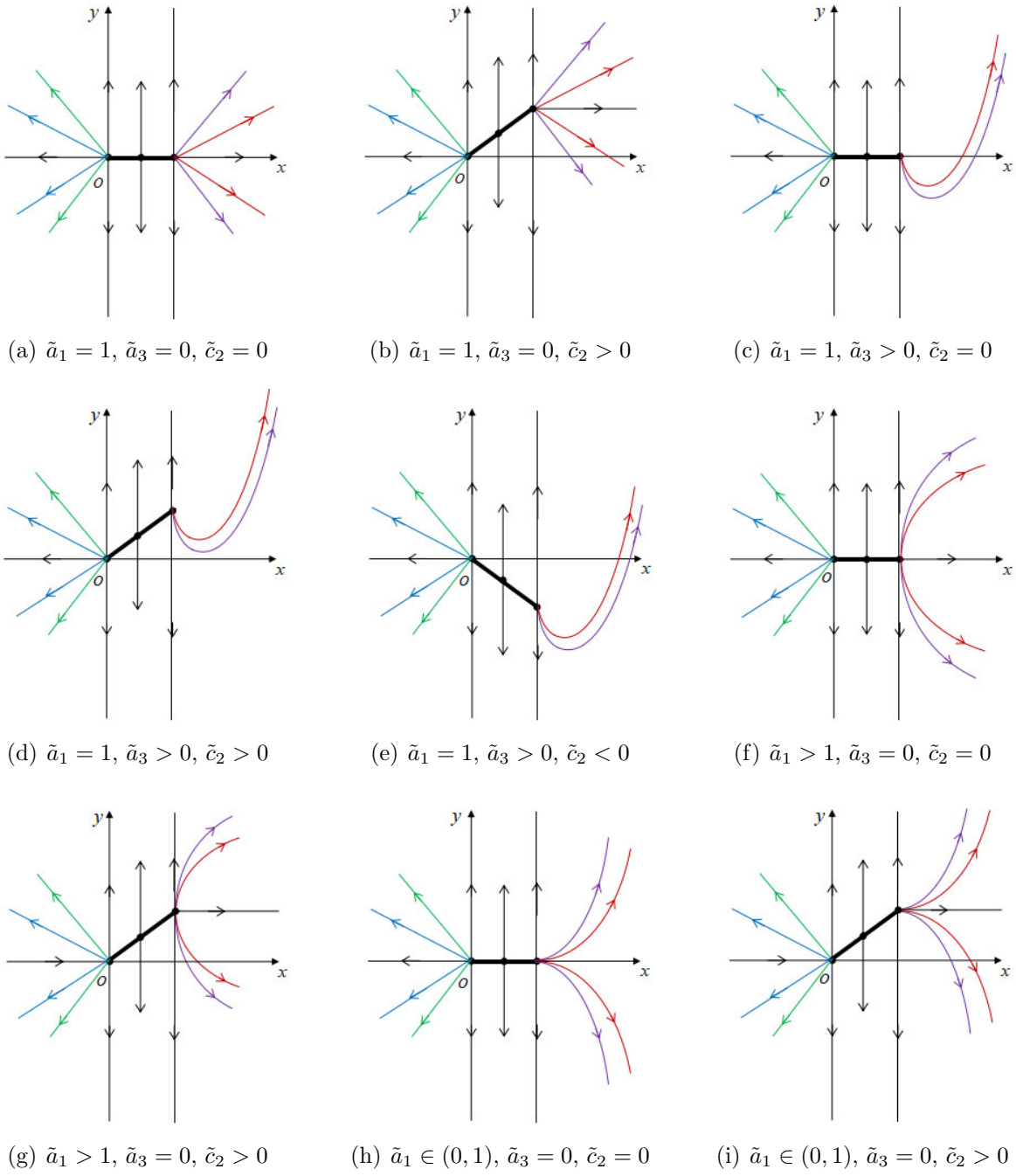

(a) $\tilde{a}_1 = 1$, $\tilde{a}_3 = 0$, $\tilde{c}_2 = 0$ (b) $\tilde{a}_1 = 1$, $\tilde{a}_3 = 0$, $\tilde{c}_2 > 0$ (c) $\tilde{a}_1 = 1$, $\tilde{a}_3 > 0$, $\tilde{c}_2 = 0$

(d) $\tilde{a}_1 = 1$, $\tilde{a}_3 > 0$, $\tilde{c}_2 > 0$ (e) $\tilde{a}_1 = 1$, $\tilde{a}_3 > 0$, $\tilde{c}_2 < 0$ (f) $\tilde{a}_1 > 1$, $\tilde{a}_3 = 0$, $\tilde{c}_2 = 0$

(g) $\tilde{a}_1 > 1$, $\tilde{a}_3 = 0$, $\tilde{c}_2 > 0$ (h) $\tilde{a}_1 \in (0,1)$, $\tilde{a}_3 = 0$, $\tilde{c}_2 = 0$ (i) $\tilde{a}_1 \in (0,1)$, $\tilde{a}_3 = 0$, $\tilde{c}_2 > 0$

Figure 18. Local phase portraits at the node-node continuum of system (27) for $\tilde{b}_1 = 1$ and $\tilde{b}_2 = 0$.

consider the case $\tilde{c}_1 \geq 0$. When $\tilde{c}_1 = 0$, according to Theorem 8, local phase portraits at the generalized boundary-focus/center points of system (30) are shown in Figure 24(a)-(c). When $\tilde{c}_1 > 0$, local phase portraits at the generalized boundary-focus/center points of system (30) are shown in Figure 24(d). □

4.7. **Indices of singular continuums.** Based on the definition of the rotation number of the continuous vector field around the oriented closed curve given in Section 2, we now introduce the definition of index for singular continuums of system (18) by considering

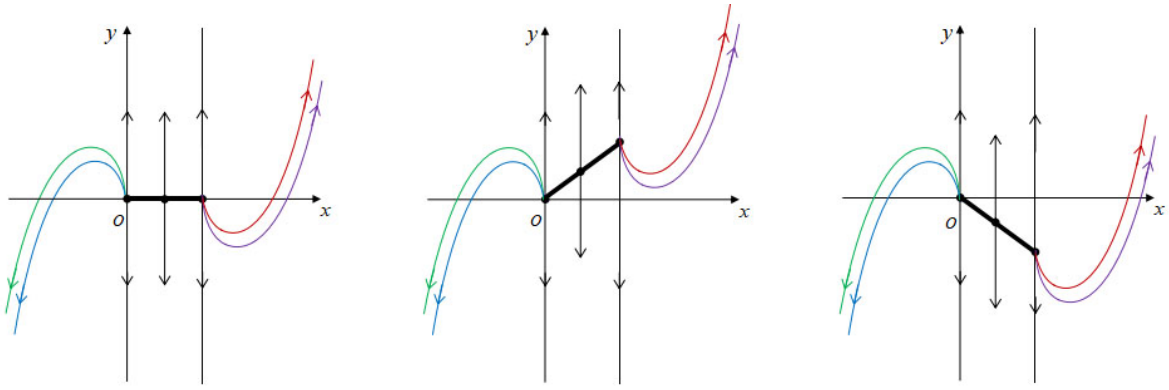

(a) $\tilde{a}_1 = 1$, $\tilde{a}_3 > 0$, $\tilde{c}_2 = 0$ (b) $\tilde{a}_1 = 1$, $\tilde{a}_3 > 0$, $\tilde{c}_2 > 0$ (c) $\tilde{a}_1 = 1$, $\tilde{a}_3 > 0$, $\tilde{c}_2 < 0$

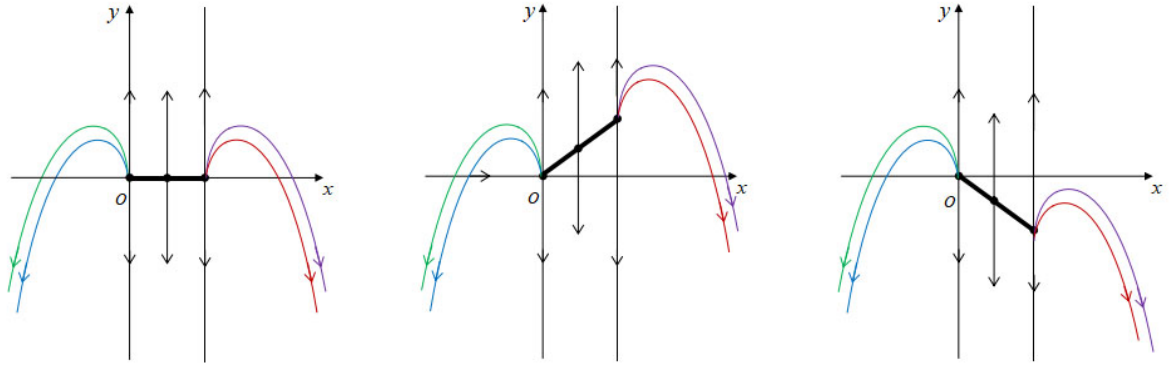

(d) $\tilde{a}_1 = 1$, $\tilde{a}_3 < 0$, $\tilde{c}_2 = 0$ (e) $\tilde{a}_1 = 1$, $\tilde{a}_3 < 0$, $\tilde{c}_2 > 0$ (f) $\tilde{a}_1 = 1$, $\tilde{a}_3 < 0$, $\tilde{c}_2 < 0$

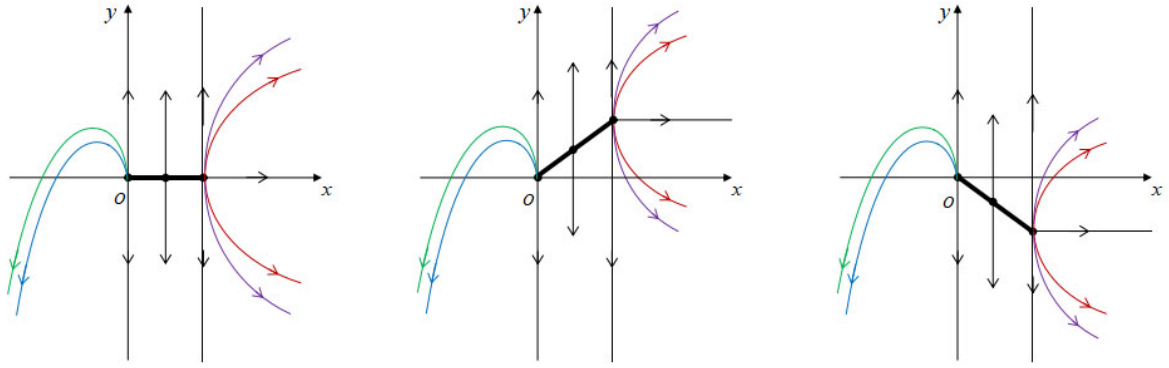

(g) $\tilde{a}_1 > 1$, $\tilde{a}_3 = 0$, $\tilde{c}_2 = 0$ (h) $\tilde{a}_1 > 1$, $\tilde{a}_3 = 0$, $\tilde{c}_2 > 0$ (i) $\tilde{a}_1 > 1$, $\tilde{a}_3 = 0$, $\tilde{c}_2 < 0$

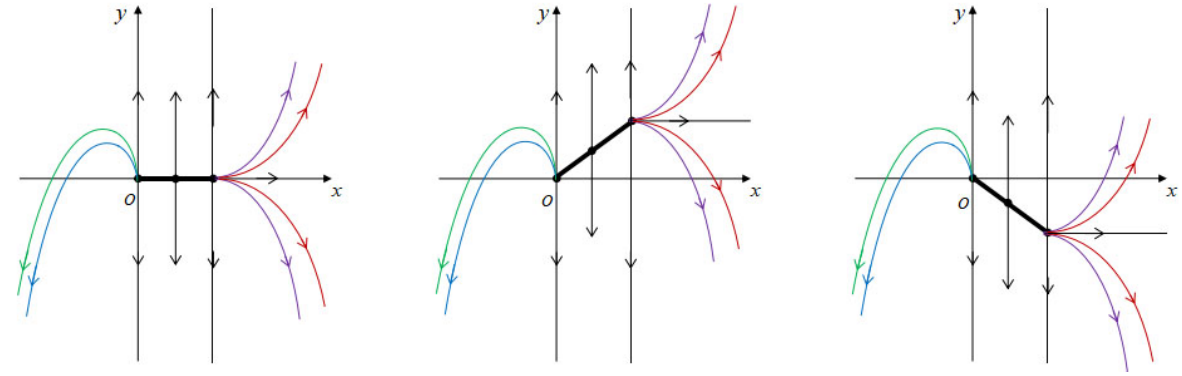

(j) $\tilde{a}_1 \in (0,1)$, $\tilde{a}_3 = 0$, $\tilde{c}_2 = 0$ (k) $\tilde{a}_1 \in (0,1)$, $\tilde{a}_3 = 0$, $\tilde{c}_2 > 0$ (l) $\tilde{a}_1 \in (0,1)$, $\tilde{a}_3 = 0$, $\tilde{c}_2 < 0$

Figure 19. Local phase portraits at the node-node continuum of system (27) for $\tilde{b}_1 = 1$ and $\tilde{b}_2 > 0$.

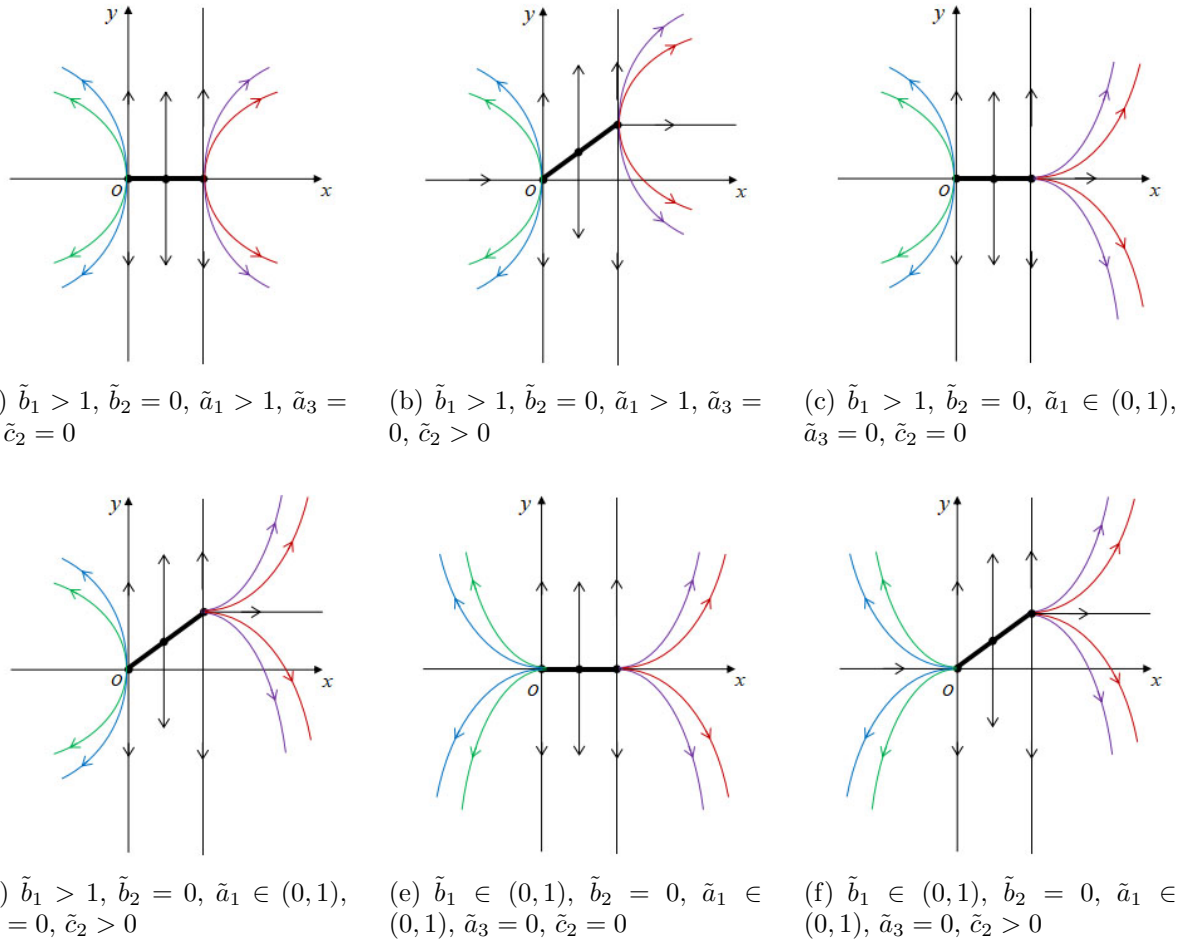

(a) $\tilde{b}_1 > 1$, $\tilde{b}_2 = 0$, $\tilde{a}_1 > 1$, $\tilde{a}_3 = 0$, $\tilde{c}_2 = 0$

(b) $\tilde{b}_1 > 1$, $\tilde{b}_2 = 0$, $\tilde{a}_1 > 1$, $\tilde{a}_3 = 0$, $\tilde{c}_2 > 0$

(c) $\tilde{b}_1 > 1$, $\tilde{b}_2 = 0$, $\tilde{a}_1 \in (0,1)$, $\tilde{a}_3 = 0$, $\tilde{c}_2 = 0$

(d) $\tilde{b}_1 > 1$, $\tilde{b}_2 = 0$, $\tilde{a}_1 \in (0,1)$, $\tilde{a}_3 = 0$, $\tilde{c}_2 > 0$

(e) $\tilde{b}_1 \in (0,1)$, $\tilde{b}_2 = 0$, $\tilde{a}_1 \in (0,1)$, $\tilde{a}_3 = 0$, $\tilde{c}_2 = 0$

(f) $\tilde{b}_1 \in (0,1)$, $\tilde{b}_2 = 0$, $\tilde{a}_1 \in (0,1)$, $\tilde{a}_3 = 0$, $\tilde{c}_2 > 0$

Figure 20. Local phase portraits at the node-node continuum of system (27) for $\tilde{b}_1 \neq 1$ and $\tilde{b}_2 = 0$.

the continuous system (18) and supposing that ω is an isolated singular continuum of system (18). Let

$$S(\omega, R) := \{(x, y) \in \mathcal{D}_2 : inf_{(u,v)\in\omega}\sqrt{(x-u)^2 + (y-v)^2} \leq R\}.$$

Then there exists a positive R such that in a sufficiently small neighborhood $S(\omega, R)$ of singular continuum ω it does not contain any equilibrium other than ω. Thus for the isolated equilibrium and any positive numbers $0 < r_1 < r_2 < R$ [20, p.147], the absence of equilibrium in the annulus $\overline{S(\omega, r_2)\backslash S(\omega, r_1)}$ implies that

$$\gamma(A_1, \partial S(\omega, r_2)) = \gamma(A_1, \partial(S(\omega, r_2)\backslash S(\omega, r_1))) + \gamma(A_1, \partial S(\omega, r_1)) = \gamma(A_1, \partial S(\omega, r_1)),$$

where$(x, y) \in \mathcal{D}_2$, $A_1(x, y) := (X_1(x, y), Y_1(x, y))$ is the vector field of system (18), and $\partial S(\omega, r)$ denotes the boundary of $S(\omega, r)$. So for $0 < r < R$, $\gamma(A_1, \partial S(\omega, r))$ is an integer independent of r.

Definition 2. *Suppose that ω is a singular continuum of system* (18)*. Let $r > 0$ be a small enough such that $S(\omega, r)$ contains ω but does not contain any other equilibrium points of system* (18)*. The rotation number $\gamma(A_1, \partial S(\omega, r))$ is called the index of the singular continuum ω of system* (18)*.*

Now we are ready to classify indices of singular continuums.

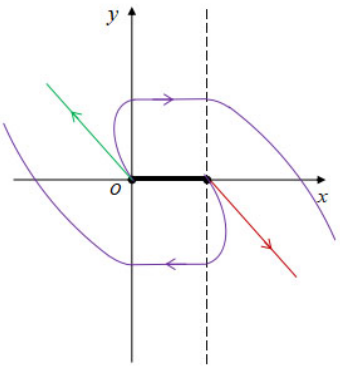

(a) $\tilde{b}_1 = 2\sqrt{-\tilde{b}_2}$, $\tilde{a}_1 = 2\sqrt{-\tilde{a}_3}$, $\tilde{c}_1 = 0$

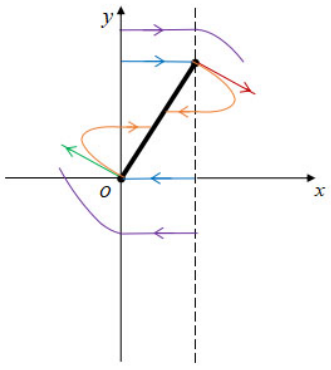

(b) $\tilde{b}_1 = 2\sqrt{-\tilde{b}_2}$, $\tilde{a}_1 = 2\sqrt{-\tilde{a}_3}$, $\tilde{c}_1 > 0$

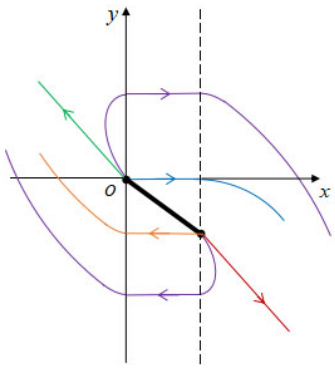

(c) $\tilde{b}_1 = 2\sqrt{-\tilde{b}_2}$, $\tilde{a}_1 = 2\sqrt{-\tilde{a}_3}$, $\tilde{c}_1 < 0$

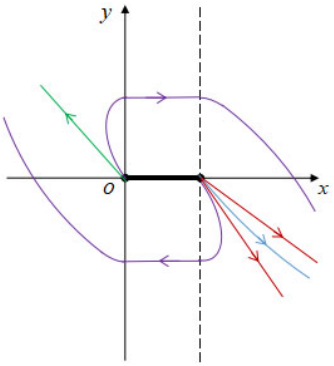

(d) $\tilde{b}_1 = 2\sqrt{-\tilde{b}_2}$, $\tilde{a}_1 > 2\sqrt{-\tilde{a}_3}$, $\tilde{c}_1 = 0$

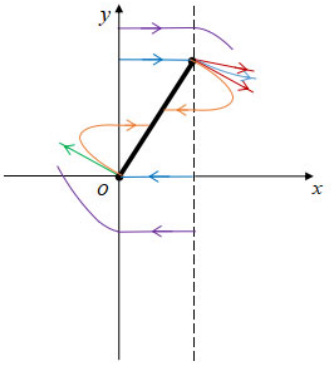

(e) $\tilde{b}_1 = 2\sqrt{-\tilde{b}_2}$, $\tilde{a}_1 > 2\sqrt{-\tilde{a}_3}$, $\tilde{c}_1 > 0$

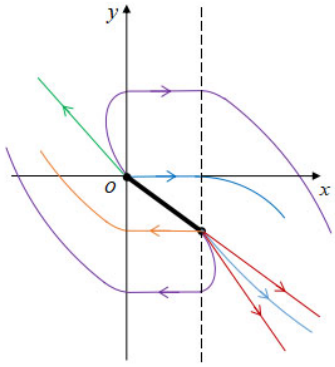

(f) $\tilde{b}_1 = 2\sqrt{-\tilde{b}_2}$, $\tilde{a}_1 > 2\sqrt{-\tilde{a}_3}$, $\tilde{c}_1 < 0$

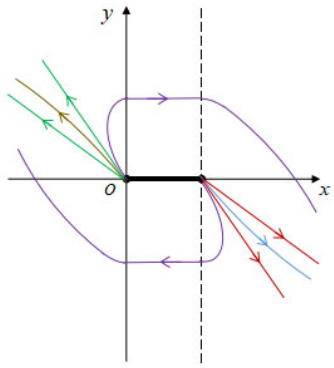

(g) $\tilde{b}_1 > 2\sqrt{-\tilde{b}_2}$, $\tilde{a}_1 > 2\sqrt{-\tilde{a}_3}$, $\tilde{c}_1 = 0$

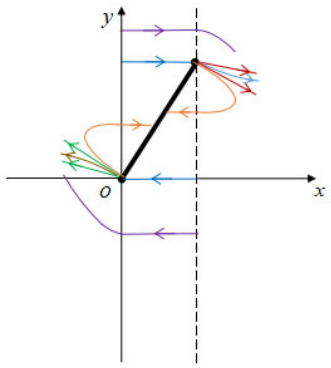

(h) $\tilde{b}_1 > 2\sqrt{-\tilde{b}_2}$, $\tilde{a}_1 > 2\sqrt{-\tilde{a}_3}$, $\tilde{c}_1 > 0$

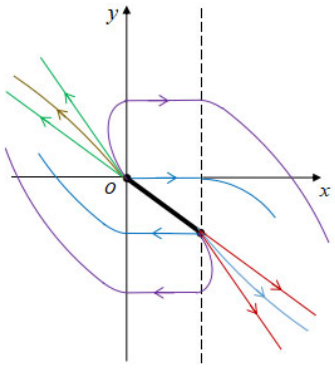

(i) $\tilde{b}_1 > 2\sqrt{-\tilde{b}_2}$, $\tilde{a}_1 > 2\sqrt{-\tilde{a}_3}$, $\tilde{c}_1 < 0$

Figure 21. Local phase portraits at the node-node continuum of system (28) for $\tilde{a}_1 \geq 2\sqrt{-\tilde{a}_3}$.

Theorem 18. *The index of an isolated singular continuum ω of system* (18) *is shown in* Table 3.

Proof. Since ω is an isolated singular continuum, there is a constant $r > 0$ satisfying Definition 2. Hence, the vector field $A_1(x, y)$ is nonsingular on $\partial S(\omega, r)$, i.e., for all

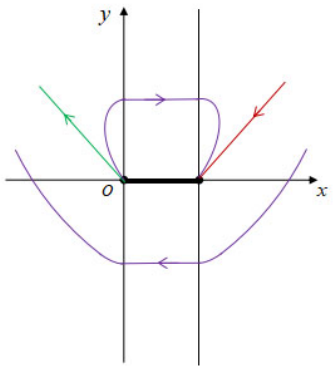

(a) $\tilde{b}_1 = 2\sqrt{-\tilde{b}_2}$, $\tilde{a}_1 = -2\sqrt{-\tilde{a}_3}$, $\tilde{c}_1 = 0$

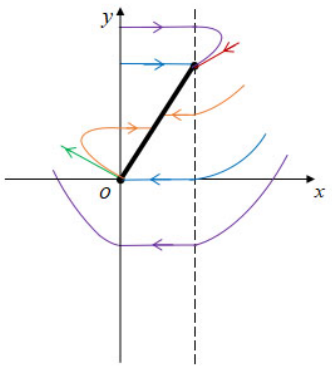

(b) $\tilde{b}_1 = 2\sqrt{-\tilde{b}_2}$, $\tilde{a}_1 = -2\sqrt{-\tilde{a}_3}$, $\tilde{c}_1 > 0$

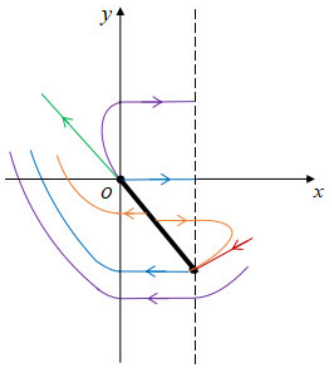

(c) $\tilde{b}_1 = 2\sqrt{-\tilde{b}_2}$, $\tilde{a}_1 = -2\sqrt{-\tilde{a}_3}$, $\tilde{c}_1 < 0$

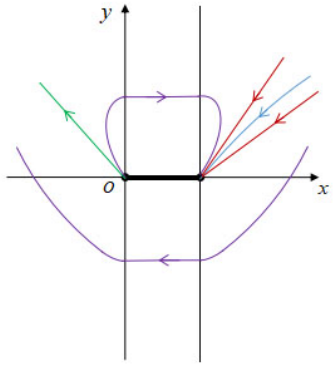

(d) $\tilde{b}_1 = 2\sqrt{-\tilde{b}_2}$, $\tilde{a}_1 < -2\sqrt{-\tilde{a}_3}$, $\tilde{c}_1 = 0$

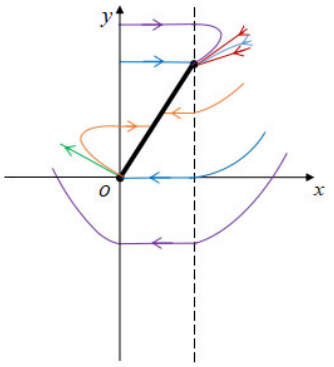

(e) $\tilde{b}_1 = 2\sqrt{-\tilde{b}_2}$, $\tilde{a}_1 < -2\sqrt{-\tilde{a}_3}$, $\tilde{c}_1 > 0$

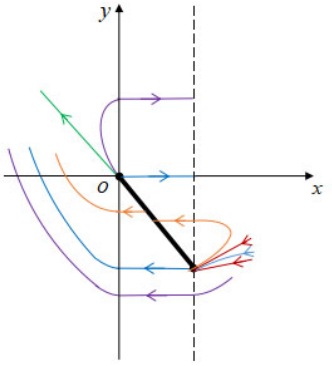

(f) $\tilde{b}_1 = 2\sqrt{-\tilde{b}_2}$, $\tilde{a}_1 < -2\sqrt{-\tilde{a}_3}$, $\tilde{c}_1 < 0$

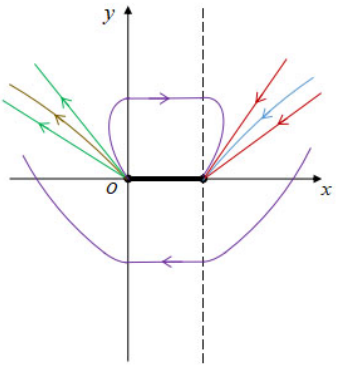

(g) $\tilde{b}_1 > 2\sqrt{-\tilde{b}_2}$, $\tilde{a}_1 < -2\sqrt{-\tilde{a}_3}$, $\tilde{c}_1 = 0$

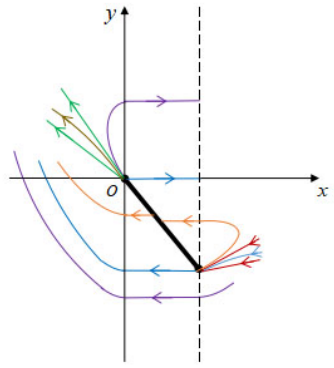

(h) $\tilde{b}_1 > 2\sqrt{-\tilde{b}_2}$, $\tilde{a}_1 < -2\sqrt{-\tilde{a}_3}$, $\tilde{c}_1 > 0$

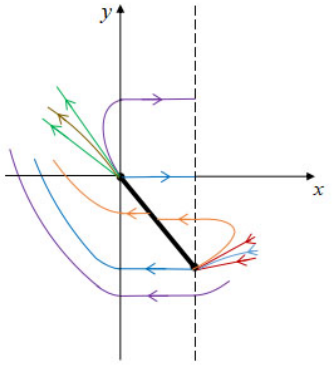

(i) $\tilde{b}_1 > 2\sqrt{-\tilde{b}_2}$, $\tilde{a}_1 < -2\sqrt{-\tilde{a}_3}$, $\tilde{c}_1 < 0$

Figure 22. Local phase portraits at the node-node continuum of system (28) for $\tilde{a}_1 \leq -2\sqrt{-\tilde{a}_3}$.

$(x', y') \in \partial S(\omega, r)$, we have $X^2(x', y') + Y^2(x', y') \neq 0$. Apparently, the vector field $A_1(x, y)$ in the $\partial S(\omega, r)$ is also piecewise smooth. For vector $A_1(x, y) = (X_1(x, y), Y_1(x, y))$ with $(x, y) \in \mathcal{S}_C \cap \partial S(\omega, r)$, we have $\arctan(Y/X) = \arctan(a_4/a_2)$ for the case $a_2 > 0$ and $\operatorname{arccot}(X/Y) = \arctan(a_2/a_4)$ for the case $a_2 = 0$, due to the assumption that a_2 and a_4 are not equal to zero simultaneously. Thus, when a point (x, y) moves along $\partial S(\omega, r)$ in the

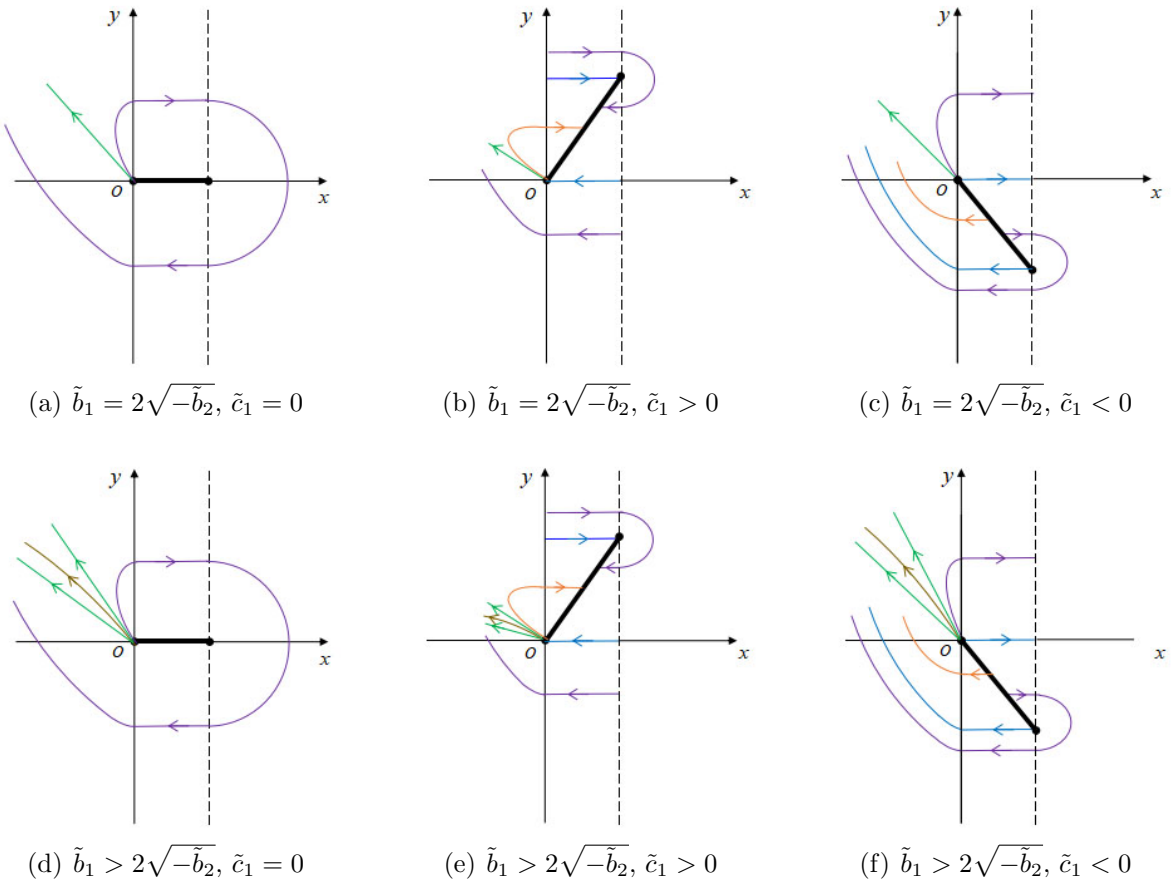

(a) $\tilde{b}_1 = 2\sqrt{-\tilde{b}_2}$, $\tilde{c}_1 = 0$ (b) $\tilde{b}_1 = 2\sqrt{-\tilde{b}_2}$, $\tilde{c}_1 > 0$ (c) $\tilde{b}_1 = 2\sqrt{-\tilde{b}_2}$, $\tilde{c}_1 < 0$

(d) $\tilde{b}_1 > 2\sqrt{-\tilde{b}_2}$, $\tilde{c}_1 = 0$ (e) $\tilde{b}_1 > 2\sqrt{-\tilde{b}_2}$, $\tilde{c}_1 > 0$ (f) $\tilde{b}_1 > 2\sqrt{-\tilde{b}_2}$, $\tilde{c}_1 < 0$

Figure 23. Local phase portraits at the node-focus continuum of system (29).

Table 3. The index of singular continuum of system (18).

Type of the singular continuum	Index
saddle-saddle continuum	-1
saddle-node continuum	0
saddle-focus continuum	
node-node continuum	1
node-focus continuum	
focus continuum	
center continuum	

counterclockwise direction, the direction variation of the vector $A(x, y)$ occurs in the zone $\overline{\mathcal{S}_C \cap \partial S(\omega, r)}$. This implies that the direction of vector $A_1(x, y)$ is only associated with the system identified in zones $\mathcal{S}_L$ and $\mathcal{S}_R$. Consequently, Table 3 follows from Theorem 10. □

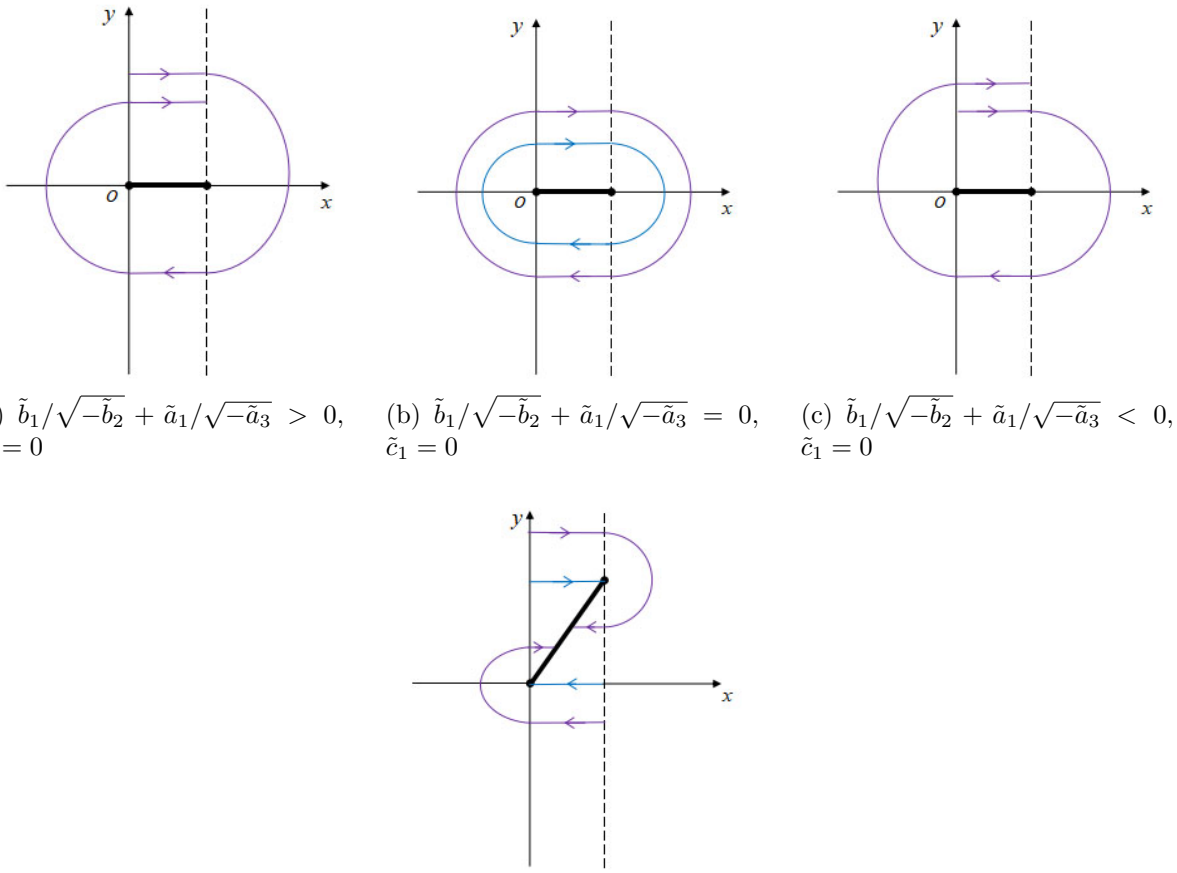

(a) $\tilde{b}_1/\sqrt{-\tilde{b}_2} + \tilde{a}_1/\sqrt{-\tilde{a}_3} > 0$, $\tilde{c}_1 = 0$

(b) $\tilde{b}_1/\sqrt{-\tilde{b}_2} + \tilde{a}_1/\sqrt{-\tilde{a}_3} = 0$, $\tilde{c}_1 = 0$

(c) $\tilde{b}_1/\sqrt{-\tilde{b}_2} + \tilde{a}_1/\sqrt{-\tilde{a}_3} < 0$, $\tilde{c}_1 = 0$

(d) $\tilde{c}_1 > 0$

Figure 24. Local phase portraits at the generalized boundary-focus/center point of system (30).

5. Concluding remarks

When a continuous linear system has only one switching line and the boundary equilibria, we note that all corresponding phase portraits of the boundary equilibria are global. When a continuous linear system has two parallel switching lines and a singular continuum, all corresponding phase portraits of the singular continuums are global except the generalized boundary-focus, because it can induce a limit cycle [3, 8]. Moreover, it is also notable that the boundary-equilibria and singular continuums may appear in the system with many parallel switching lines.

When a continuous linear system has only one boundary equilibrium or one singular continuum, the necessary condition of the existence of limit cycle is that the index of the boundary equilibrium or singular continuum is 1. According to Theorem 10, for boundary equilibria, there includes boundary-node, boundary-focus, boundary-center, and node-focus. Based on Theorem 18, for singular continuum, there includes node-node continuum, node-focus continuum, focus continuum and center continuum. It is notable that the index of a singular continuum which intersects one or more than one parallel switching lines are the same as the one which does not intersect any switching lines given in Theorem 18. However, it is difficult to show local phase portraits for such singular continuums at this stage since these singular continuums are polyline segments.

Acknowledgements

The first and third authors are supported by National Natural Science Foundation of China No. 12171485, the second author is supported by NSF DMS-1820771 and the fourth author is supported by National Natural Science Foundation of China No. 12171337.

Data Availability

All data, models and code generated or used during the study appear in the submitted article.

Conflict of interest

The authors declare that they have no conflict of interest.

Disclosure of potential conflicts of interest-ethical and financial

The authors declare that they have no known competing financial interests or personal relationships that could have appeared to influence the work reported in this paper.

References

[1] M. di Bernardo, C.J. Budd, A.R. Champneys, P. Kowalczyk, *Piecewise-smooth Dynamical Systems: Theory and Applications*, Springer-Verlag, London, 2008.
[2] M. di Bernardo, C.J. Budd, A.R. Champneys, P. Kowalczyk, A.B. Nordmark, G. Olivar Tost, P.T. Piiroinen, *Bifurcations in nonsmooth dynamical systems*, *SIAM Review* **50** (2008), 629-701.
[3] H. Chen, Y. Tang, A proof of Euzébio-Pazim-Ponce's conjectures for a degenerate planar piecewise linear differential system with three zones, *Phys. D* **401** (2020), 132150, 1–22.
[4] H. Chen, M. Jia, Y. Tang, A degenerate planar piecewise linear differential system with three zones, *J. Differential Equations* **297** (2021), 433-468.
[5] F. Corinto, A. Ascoli, M. Gilli, Nonlinear dynamics of memristor oscillators, *IEEE Trans. Circuit Syst. -I* **58** (2011), 1323-1336.
[6] M. Desroches, A. Guillamon, E. Ponce, R. Prohens, S. Rodrigues, A. Teruel, Canards, folded nodes, and mixed-mode oscillations in piecewise-linear slow-fast systems, *SIAM Review* **58** (2016), 653-691.
[7] F. Dumortier, J. Llibre, J.C. Artés, *Qualitative Theory of Planar Differential Systems*, UniversiText, Springer-Verlag, New York, 2006.
[8] R. Euzébio, R. Pazim, E. Ponce, Jump bifurcations in some degenerate planar piecewise linear differential systems with three zones, *Physica D* **325** (2016), 74-85.
[9] E. Freire, E. Ponce, F. Rodrigo, F. Torres, Bifurcation sets of continuous piecewise linear systems with two zones, *Int. J. Bifurcation and Chaos* **8** (1998), 2073-2097.
[10] S.J. Hogan, M.E. Homer, M.R. Jeffrey, R. Szalai, Piecewise smooth dynamical systems theory: The case of the missing boundary equilibrium bifurcations, *J. Nonlinear Sci.* **26** (2016), 1161-1173.
[11] M.R. Jeffrey, The ghosts of departed quantities in switches and transitions, *SIAM Review* **60** (2018), 116-136.
[12] M.R. Jeffrey, S.J. Hogan, The geometry of generic sliding bifurcations, *SIAM Review* **53** (2011), 505-525.
[13] S. Lefschetz, *Differential Equations: Geometric Theory*, Pure and Applied Mathematics, Interscience Publishers, New York, 1963.
[14] S. Li, J. Llibre, Phase portraits of piecewise linear continuous differential systems with two zones separated by a straight line, *J. Differential Equations* **266** (2019), 8094–8109.
[15] J. Llibre, E. Ponce, C. Valls, Uniqueness and non-uniqueness of limit cycles for piecewise linear differential systems with three zones and no symmetry, *J. Nonlinear Sci.* **25** (2015), 861–887.
[16] J. Llibre, E. Ponce, C. Valls, Two limit cycles in Liénard piecewise linear differential systems, *J. Nonlinear Sci.* **29** (2019), 1499–1522.

[17] H.P. McKean, Nagumo's equation, *Adv. Math.*, **4** (1970), 209-223.
[18] H.P. McKean, Stabilization of solutions of a caricature of the Fitzhugh-Nagumo equation, *Comm. Pure. Appl. Math.*, **36** (1983), 291-324.
[19] D.B. Strukov, G.S. Snider, D.R. Stewart, R.S. Williams, The missing memristor found, *Nature*, **453** (2008), 80-83.
[20] Z. Zhang, T. Ding, W. Huang, Z. Dong, *Qualitative Theory of Differential Equations*, Transl. Math. Monogr., Amer. Math. Soc., Providence, RI, 1992.

[1]School of Mathematics and Statistics, HNP-LAMA, Central South University, Changsha, Hunan 410083, China

Email address: chen_hebai@csu.edu.cn (Chen); y_ang_hao@163.com (Yang)

[2]School of Mathematical and Statistical Sciences, University of Texas Rio Grande Valley, Edinburg, TX 78539, USA

Email address: zhaosheng.feng@utrgv.edu (Feng)

[3]School of Mathematics, Sichuan University, Chengdu, Sichuan 610064, China

Email address: zlf63math@163.com; zlf63math@scu.edu.cn (Zhou)